

A unifying view of Gamma–Ray Burst Afterglows

G. Ghisellini^{1*}, M. Nardini², G. Ghirlanda¹ and A. Celotti².

¹INAF – Osservatorio Astronomico di Brera, Via Bianchi 46 I–23806 Merate, Italy

²SISSA – Via Beirut 2/4, I–34014 Trieste, Italy

5 November 2021

ABSTRACT

We selected a sample of 33 Gamma–Ray Bursts (GRBs) detected by *Swift*, with known redshift and optical extinction at the host frame. For these, we constructed the de–absorbed and K–corrected X–ray and optical rest frame light curves. These are modelled as the sum of two components: emission from the forward shock due to the interaction of a fireball with the circum–burst medium and an additional component, treated in a completely phenomenological way. The latter can be identified, among other possibilities, as “late prompt” emission produced by a long lived central engine with mechanisms similar to those responsible for the production of the “standard” early prompt radiation. Apart from flares or re–brightenings, that we do not model, we find a good agreement with the data, despite of their complexity and diversity. Although based in part on a phenomenological model with a relatively large number of free parameters, we believe that our findings are a first step towards the construction of a more physical scenario. Our approach allows us to interpret the behaviour of the optical and X–ray afterglows in a coherent way, by a relatively simple scenario. Within this context it is possible to explain why sometimes no jet break is observed; why, even if a jet break is observed, it is often chromatic; why the steepening after the jet break time is often shallower than predicted. Finally, the decay slope of the late prompt emission after the shallow phase is found to be remarkably similar to the time profile expected by the accretion rate of fall–back material (i.e. $\propto t^{-5/3}$), suggesting that this can be the reason why the central engine can be active for a long time.

Key words: gamma–ray: bursts — radiation mechanisms: non–thermal — X–rays: general

1 INTRODUCTION

The GRB X–ray light curves, as observed by *Swift*, have shown a complexity unforeseen before. Besides the behaviour as observed by *BeppoSAX* after several hours from the trigger, a significant fraction of GRBs shows a steep flux decay soon after the end of the prompt as seen by BAT, followed by a plateau lasting for a few thousands seconds, ending at the time T_A (following Willingale et al. 2007). This trend, named “Steep–Flat–Steep” (Tagliaferri et al. 2005; Nousek et al. 2006) has been interpreted in several ways (for a recent review see e.g. Zhang 2007). Furthermore, in nearly half of the bursts, X–ray flares, of relatively short duration Δt , i.e. $\Delta t/t \sim 0.1$, (e.g. Chincarini et al. 2007) are observed even several hours after the trigger. Considering X–ray flares in different GRBs, Lazzati, Perna & Begelman (2008) have shown that their average luminosity decays as $t^{-5/3}$, similarly to what predicted following the mass accretion rate of fall–back material (see Chevalier 1989; Zhang, Woosley & Heger 2008).

The optical light curves are also complex, but rarely track the X–ray flux behaviour (see e.g. Panaitescu et al. 2006, Panaitescu 2007a, Panaitescu 2007b), suggesting a possible different origin.

For 10–15 per cent of bursts, precursor emission is detected, preceding the main event in some cases by hundreds of seconds. The energy contained in the precursors is comparable to that in the main event, and the spectra in the two phases are indistinguishable (Burlon et al. 2008), suggesting that they are produced by the same mechanism.

Much theoretical effort has been made to understand the “Steep–Flat–Steep” behaviour, shown especially by the X–ray light curve. The initial steep decay is interpreted as “curvature” (or “high latitude”) emission of the fireball: when the prompt ceases, the emission is dominated by radiation produced from parts of the fireball not exactly pointing at us (Zhang et al. 2006; Nousek et al. 2006, but see e.g. Peer, Mészáros & Rees 2006 for an alternative interpretation). At later times, the relatively steep decay observed after T_A is generally explained as the “standard” forward (external) shock emission, namely as corresponding to the X–ray afterglow phase typically observed by *BeppoSAX* several hours after the burst trigger. There are however some alternative interpretations (see below). The most puzzling phase is the shallow, or plateau, one. Several models have been proposed, aiming at accounting not only for the shallow flux decay but also why it steepens at the break time T_A . The proposed alternative interpretations include:

* Email: gabriele.ghisellini@brera.inaf.it

- Energy injection. Zhang et al. (2006) propose that the shallow decay can be produced by a continuous, long-lasting, energy injection into the forward external shock. There are at least two possibilities, depending on whether the central engine is long or short lived. A long-lived engine could have luminosity that smoothly decreases as $L(t) \propto t^{-q}$ with $q < 1$ (Zhang et al. 2006; Zhang & Meszaros 2001), with T_A corresponding to the end of the energy injection phase.

A short-lived engine (i.e. of duration comparable to that of the prompt phase) can produce shells with a steep power-law distribution of Γ factors. T_A is determined by a cutoff in the Lorentz factor distribution. The two alternatives cannot be currently distinguished observationally. Both interpret the plateau as afterglow emission from a continuously refreshed shock. The required energetic (in bulk motion) largely exceeds what required to produce the prompt emission.

- Reverse shocks. The shallow decay could be produced as synchrotron emission from the reverse external shock if the micro-physical parameters ϵ_e and ϵ_B are much larger than those in the forward shock. In this situation the ratio of the X-ray flux produced by the reverse and forward shocks would be dominated by the former. Along these lines Uhm & Beloborodov (2007) and Genet, Daigne & Mochkovitch (2007) suggested that the X-ray plateau emission is due to the reverse shock running into ejecta of relatively small (and decreasing) Lorentz factors. This requires an appropriate Γ distribution of the ejecta, besides the suppression of the X-ray flux produced by the forward shock.

- Time dependent micro-physical parameters. If the relativistic electron distribution has a typical slope $p \sim 2$, the X-ray luminosity is proportional to the bolometric luminosity ($L_X = \epsilon_e L_{bol}$). Since $L_{bol} \propto t^{-1}$, a time evolution of $\epsilon_e \propto t^{1/2}$ would produce $L_X \propto t^{-1/2}$, close to the observed plateau slopes. T_A is identified with the time ϵ_e reaches its maximum value (~ 0.1) (Ioka et al. 2006).

- Precursor fireball (Ioka et al. 2006). In this scenario a precursor, occurring 10^3 – 10^6 s before the main burst, generates a first fireball with low Γ , whose afterglow is too faint to be detected. The main burst then generates another, more powerful, fireball with a larger Γ . This second fireball, interacting with the first one, produces the plateau phase. When the two fireballs merge and interact with the circum-burst medium, the standard afterglow sets in.

- Up-scattering of forward shock photons. Panaitescu (2008) suggested that a relativistic shell would scatter protons produced by a forward shock located ahead of it. While this occurs also if the relativistic shell does not dissipate (bulk Compton), the process is more effective if dissipation (through, e.g. internal shocks) occurs, heating the electrons of the shell. The up-scattered component is expected to be more relevant in X-rays than in optical, thus overshining the standard afterglow (i.e. forward shock) more easily in the X-ray band.

- Geometrical models. If two co-aligned jets, with different opening angles, are observed at an angle θ_v within the wide cone, but outside the narrow one, the emission from the narrow jet would be visible only once it has decelerated. The observed light curve of the afterglow of the narrow jet would be flat before T_A , mimicking the observed plateau (see e.g. Racusin et al. 2008 for the case of GRB 080319B). In this model the time T_A is the time at which the Lorentz factor Γ of the narrow jet decreases to $\sim 1/\theta_v$. A somewhat similar model is the off-beam model by Eichler & Granot (2006) in which the shallow phase represents the smooth peak of an afterglow observed off-axis. Here too T_A is identified by the time when the whole jet emission becomes visible.

In the patchy shell model, Toma et al. (2006) propose that the early X-ray afterglow could be produced by an inhomogeneous jet of aperture angle ~ 0.1 rad composed by multiple sub-jets subtending a smaller aperture ($\theta_{s-j} < 0.01$ rad). The latter ones are observable when their Γ decelerate to $\sim 1/\theta_v$. A shallow phase is ascribed to the superposition of the single sub-jet emissions, seen by an observer not exactly on-axis with any of them. When they merge due to sideways expansion the normal afterglow begins to dominate: this corresponds to the time T_A . Therefore the duration of the shallow phase depends on the (still uncertain) sideways expansion velocity.

- Dust scattering. Shao & Dai (2007) interpret the plateau as prompt X-ray flux scattered by dust grains located in the burst surroundings (within ~ 100 pc). This model has been recently questioned by Shao et al. (2008) as it predicts a strong spectral softening during the shallow decay phase, inconsistent with the data. Moreover, the large amount of dust required would imply an optical extinction in excess of what observed.

- Cannonballs. Dado, Dar & De Rújula (2005) propose that the entire steep-flat-steep behaviour of the X-ray light curve is due the sum of thermal bremsstrahlung and synchrotron emission from a cannonball decelerating in the circum-burst medium. The time T_A would correspond to the start of the deceleration phase.

- Ruffini et al. (2008) explain the early prompt and the steep-flat-steep phases within a unique scenario, a baryonic shell (fireshell) interacting with a non-homogeneous circum-burst medium. The emission process is thermal at all times. Once the fireshell reaches a region of low density, ~ 0.03 – 2 pc away, it would decelerate very slowly, giving origin to the plateau phase.

It should be noted that the shallow phase is not ubiquitous: there are X-ray afterglows light curves where it is not detected. Therefore, any viable model should explain also the variety of the X-ray flux time behaviour. More importantly, all the above models propose that the X-ray shallow phase is due to afterglow emission (with the exception of the upscattering model by Panaitescu 2008). Thus, the same forward (or reverse) shock should produce optical radiation, which presumably would track the X-ray flux trend, including the shallow decay phase. This is not observed for some bursts which, therefore, challenge the above interpretation.

Ghisellini et al. (2007) instead suggested that the plateau phase of the X-ray (and sometimes optical) emission corresponds to a “late prompt”, namely due to the prolonged activity of the central engine (see also Lazzati & Perna 2007): after an early “standard” prompt, the engine keeps producing shells of progressively lower power and bulk Lorentz factor for a long time (i.e. days). The dissipation during this and the early phases occurs at similar distances (close to the transparency radius). The reason for the shallow decay phase, and for the break ending it, is that the Γ -factors of the late shells are monotonically decreasing, allowing to see an increasing portion of the emitting surface, until all of it is visible. The break at T_A occurs when $\Gamma(t) = 1/\theta_j$. In our scenario two independent emission components compete: the prevailing of the “late prompt” vs a standard afterglow emission at different times can account for the variety of behaviours of X-ray and optical fluxes.

In this work we thus try to model simultaneously both the X-ray and optical light curves as the sum of two components. The first one is the emission produced by the forward shock, according to the standard afterglow modelling. The second one is simply parametrised, spectrally and temporally. Though we refer to it as “late prompt” emission (which reflects our proposal), such a component could correspond to other interpretations. One of the aim

of our investigation is to find the constraints that a more physical model must satisfy to give origin to this “late prompt” component.

Throughout this paper, a Λ CDM cosmology with $\Omega_M = 0.3$ and $\Omega_\Lambda = h = 0.7$ is adopted.

2 THE SAMPLE

All *Swift* bursts with known redshift, optical and X-ray follow up, as of end of March 2008, were considered. Among them, we selected GRBs for which an estimate of the optical extinction at the host site appeared in literature¹. This criterion is dictated by the need to determine reliable optical and X-ray intrinsic luminosities, in order to model their time dependent behaviour. The corresponding sample comprises 33 bursts.

Information concerning these 33 GRBs are listed in Table 1, where we report: redshift, A_V^{host} , optical spectral indices β_o (corrected for extinction), X-ray spectral indices β_X (again accounting for absorption), hydrogen column density N_H^{host} (at the host) as determined by fitting the X-ray spectrum.

It should be noted that usually A_V^{host} is determined by requiring that the intrinsic optical spectrum is a power-law, and correcting the observed spectral curvature according to an extinction curve (the Small Magellanic Cloud one in most cases). Sometimes however, the requirement adopted was that the optical and X-ray data lie on the same functional curve (being it a single or a broken power-law). When multiple choices were available, estimates based on the optical data alone were preferred as the X-ray flux could belong to a different spectral component. For details on the host frame dust absorption determination for each GRB see the references in Table 1.

In order to compare the behaviour of different bursts we dereddened the observed optical fluxes taking into account both the GRB host dust and the Galactic (Schlegel, Finkbeiner & Davis 1998) absorption along the line of sight. The reddening corrected fluxes have been then K-corrected and converted into monochromatic luminosities through:

$$L(\nu_0) = \frac{4\pi d_L^2}{(1+z)^{1-\beta_o}} F(\nu_0), \quad (1)$$

where ν_0 is the central frequency of the photometric filter, d_L is the luminosity distance and β_o is the unabsorbed optical spectral index (see Table 1).

The X-ray light curves were taken from the UK Swift Science Data Centre² (see Evans et al. 2007 describing how the data were reduced). Also the X-ray 0.3-10 keV XRT light curves have been corrected for the combined effects of both host frame N_H and Galactic column densities, using the unabsorbed spectral index β_X obtained from the X-ray spectral analysis (see Table 1). The unabsorbed 0.3–10 keV observer frame fluxes F_X have been converted to host frame 0.3-10 keV luminosities L_X as:

$$L_X = \frac{4\pi d_L^2}{(1+z)^{1-\beta_X}} F_X. \quad (2)$$

For simplicity, we use the same β_X for the entire X-ray light curve, neglecting the sudden changes of β_X sometimes seen during X-ray flares, since the interpretation of the individual flares is beyond the aim of this work. The analysis has been carried on in the GRB host

time frame. We therefore rescale all the observed time intervals by $(1+z)^{-1}$.

3 THE MODEL

As mentioned we assume that at all times the flux is the sum of two components: the first one due to synchrotron radiation produced by the standard forward shock caused by the fireball running into the circum-burst material; the second one is treated phenomenologically, since its form/origin is not currently known, though it can be possibly ascribed to the extension in time of the early prompt emission.

3.1 Forward shock component

Following the analytical prescriptions of Panaitescu & Kumar (2000) the forward shock emission depends on the following parameters:

- (i) E_0 — the (isotropic equivalent) kinetic energy of the fireball after it has produced the early prompt radiation;
- (ii) Γ_0 — the initial fireball bulk Lorentz factor. It controls the onset of the afterglow, but it does not influence the rest of the light curve. It is then rather undetermined when very early data are not available;
- (iii) n_0 or \dot{M}_w/v_w — n_0 is the value of the circum-burst medium density if homogeneous, while \dot{M}_w/v_w (wind mass loss rate over the wind velocity) determines the normalisation of the density in the wind case ($\propto R^{-2}$) profile;
- (iv) ϵ_e — the “equipartition” parameter setting the fraction of the available energy responsible for electron acceleration;
- (v) ϵ_B — the “equipartition” parameter parametrizing the fraction of the available energy which amplifies the magnetic field;
- (vi) p — the slope of the relativistic electron energy distribution, as injected at the shock.

For simplicity, we assume that higher frequency of the afterglow synchrotron emission is beyond the X-ray range. These are 6 free parameters, if we consider n_0 or \dot{M}_w/v_w as a single one: in reality, the assumed homogeneous vs wind-like density profile can be considered as an additional degree of freedom.

3.2 Late prompt component

In the absence of a clear understanding of its origin, this component is parametrised with the only criterion of minimising the number of free parameters. This can be considered as a first step towards a more physical modelling of this second component. A subsequent analysis of the parameters distribution could help us in constraining possible theoretical ideas. A first attempt in this direction will be discussed in §5.

The spectral shape – assumed to be constant in time – is described by a broken power-law:

$$\begin{aligned} L_L(\nu, t) &= L_0(t) \nu^{-\beta_X}; & \nu > \nu_b \\ L_L(\nu, t) &= L_0(t) \nu_b^{\beta_o - \beta_X} \nu^{-\beta_o}; & \nu \leq \nu_b, \end{aligned} \quad (3)$$

where L_0 is a normalisation constant. L_0 is not treated as a free parameter by taking it as the 0.3–10 keV luminosity L_{LX} of the late prompt emission at the time T_A :

$$L_{LX}(T_A) = \int_{0.3}^{10} L_L(\nu, T_A) d\nu \quad (4)$$

¹ For one of them, GRB 070802, the photometric data set is not yet available

² http://www.swift.ac.uk/xrt_curves/

GRB	z	A_V^{host}	β_o	β_X	N_H^{host}	$\log E_{\text{iso}}$	T_{90}	Ref
050318	1.44	0.68±0.36	1.1±0.1	1.09±0.25	0.4±0.1	52.11	32	Ber05a, Sti05, Per05
050319	3.24	0.11	0.59	0.73±0.05	3.8±2.2	52.31	152.5	Fyn05a, Kan08, Cus06
050401	2.8992	0.62±0.06	0.5±0.2	0.89±0.03	16.0±3	53.47	33.3	Fyn05b, Wat06, Wat06
050408	1.2357	0.73±0.18	0.28±0.33	1.1±0.1	12.0±3.5	52.18	15	Ber05b, DUP07, Cap07
050416A	0.653	0.19±0.11	1.14±0.2	1.04±0.05	6.8±1.0	50.69	2.5	Cen05, Hol07, Man07a
050525A	0.606	0.32±0.2	0.57±0.29	1.1±0.25	1.5±0.7	52.94	8.8	Fol05, Kan08, Blu06
050730	3.967	0	0.56±0.06	0.87±0.02	6.8±1	53.19	156.5	Che05, Pan06, Per07
050801	1.56	0	0.6	0.87±0.23	0±0.5	51.25	19.4	DeP07, Kan08, DeP07
050802	1.71	0.55±0.1	0.72±0.04	0.88±0.04	2.8±0.5	52.16	19.0	Fyn05d Sch07, Oat07
050820A	2.612	0	0.77±0.08	0.94±0.07	6±4	53.17	26.0	Pro05, Cen06a, Pag05
050824	0.83	0.14±0.13	0.45±0.18	1.0±0.1	1.8±0.65	50.68	22.6	Fyn05f, Kan08, Sol07
050922C	2.198	0	0.51±0.05	0.89±0.16	0.65±0.27	52.98	4.5	Jak05a, Kan08, Sch05
051111	1.55	0.39±0.11	1.1±0.06	1.15±0.15	8±3	52.43	46.1	Hil05, Sch07, Gui07
060124	2.296	0	0.73±0.08	1.06±0.06	13±4.5	53.6	750	Cen06b, Mis07, Rom06
060206	4.045	0±0.02	0.73±0.05	1.0±0.3	0.4±0.3	52.48	7.6	Fyn06, Kan08, Mor06
060210	3.91	1.14±0.2	1.14±0.03	1.14±0.03	100±12	53.14	255.	Cuc06, Cur07b, Cur07b
060418	1.489	0.25±0.22	0.29±0.04	1.04±0.13	1.0±0.4	52.72	103.1	Pro06, Ell06, Fal06
060512	0.4428	0.44±0.05	0.99±0.02	0.99±0.02	0	50.12	8.5	Blo06, Sch07, Sch07
060526	3.221	0.04±0.04	0.495±0.144	0.8±0.2	0	52.43	298.2	Ber06, Thö08, Cam06
060614	0.125	0.05±0.02	0.81±0.08	0.84±0.08	0.15±0.12	50.96	108.7	Pri06, Man07b, Man07b
060729	0.54	1.05	1.1	1.11±0.01	1.9±0.4	51.37	115.3	Thö06, Gru07, Gru07
060904B	0.703	0.44±0.05	0.90±0.04	1.16±0.04	4.09±0.13	51.40	171.5	Fug06, Kan08, Gru06
060908	2.43	0.055±0.033	0.69	0.95±0.15	0.64±0.34	52.66	19.3	Rol06, Kan08, Eva06
060927	5.47	0.33±0.18	0.64±0.2	0.87	<0.34	52.82	22.5	Fyn06c, RuV07, RuV07
061007	1.26	0.48±0.19	1.02±0.05	1.01±0.03	5.8±0.4	53.33	75.3	Osi06, Mun07, Mun07
061121	1.314	0.72±0.06	0.62±0.03	0.87±0.08	9.2±1.2	52.85	81.3	Blo06, Pag07, Pag07
061126	1.1588	0	0.93±0.02	1.00±0.07	11±0.7	53.08	70.8	Per08a, Per08a, Per08a
070110	2.352	0.08	1.1±0.1	1.1±0.1	2.6±1.1	52.37	88.4	Jau07, Tro07, Tro07
070125	1.547	0.11±0.4	0.58±0.1	1.1±0.1	2±1	54.08	65	Fox07, Kan08, Upd08
071003	1.1	0.209±0.08	0.93±0.04	1.14±0.12	1.1±0.4	52.28	150	Per07, Per08b, Per08b
071010A	0.98	0.615±0.15	0.76±0.25	1.46±0.2	17.4±4.5	50.7	6	Pro07, Cov08a, Cov08a
080310	2.42	0.1±0.05	0.6	0.9±0.2	7.0±1	52.49	365	Pro08, PeB08, Bea08
080319B	0.937	0.07±0.06	0.33±0.04	0.814±0.013	1.87±0.13	53.27	50	Vre08, Blo08, Blo08

Table 1. The sample. For all bursts we report information taken from the literature (see the references), namely: redshift, optical extinction and hydrogen column density at the host (A_V^{host} and N_H^{host} , respectively), and the optical and X-ray indices found after de-absorbing. E_{iso} is in the 15-150 keV band, not K-corrected. T_{90} is in seconds, from the Swift catalogue (<http://swift.gsfc.nasa.gov/docs/swift/archive/grbtable.html/>). References: Ber05a: Berger et al. (2005a); Sti05: Still et al. (2005); Per05: Perri et al. (2005); Fyn05a: Fynbo et al. (2005a); Kan08: Kann et al. (2008); Cus06: Cusumano et al. (2006); Fyn06: Fynbo et al. (2005b); Wat06: Watson et al. (2006); Ber05b: Berger et al. (2005b); DUP07: importantde Ugarte Postigo (2007); Cap07: Capalbi et al. (2007); Cen05: Cenko et al. (2005); Hol07: Holland et al. (2007); Man07a: Mangano et al. (2007a); Fol05: Foley et al. (2005); Blu06: Blustin et al. (2006); Che05: Chen et al. (2005); Pan06: Pandey et al. (2006); Per06: Perri et al. (2007); DeP07: de Pasquale et al. (2007); Fyn05d: Fynbo et al. (2005d); Sch07: Schady et al. (2007); Oat07: Oates et al. (2007); Pro05: Prochaska et al. (2005); Cen06a: Cenko et al. (2006a); Pag05: Page et al. (2005); Fyn05f: Fynbo et al. (2008f); Sol07: Sollerman et al., (2007); Jak05a: Jakobsson et al. (2005a); Ken05: Kennea et al. (2005); Hil05: Hill et al. (2005); Gui07: Guidorzi et al. (2007); Cen06b: Cenko et al. (2006b); Rom06: Romano et al. (2006); Fyn06: Fynbo et al. (2006a); Mor06: Morris et al. (2006); Cuc06: Cucchiara Fox & Berger (2006); Cur07b: Curran et al. (2007b); Pro06: Prochaska et al. (2006); Ell06: Ellison et al. (2006); Fal06: Falcone et al. (2006); Blo06: Bloom et al. (2006); Ber06: Berger & Gladders (2006); Tho08: Thöne et al. (2008), Cam06: Campana et al. (2006a); Pri06: Price Berger & Fox (2006); Man07b: Mangano et al., (2007b); Thö06: Thöne et al., (2006); Gru07: Grupe et al. (2007); Fug06: Fugazza et al. (2006); Gru06: Grupe et al. (2006); Rol06: Rol et al. (2006); Eva06: Evans et al., (2006); Fyn06c: Fynbo et al. (2006c); RuV07: Ruiz-Velasco et al., (2007); Osi06: Osip Chen & Prochaska (2006); Mun07: Mundell et al. (2007); Blo06: Bloom Perley & Chen (2006), Pag07: Page et al. (2007); Per08a: Perley et al. (2008a); Jau07: Jaunsen et al. (2007); Tro07: Troja et al. (2007); Fox et al. (2007); Upd08: Updike et al. (2008); Per07: Perley et al. (2007); Per08b: Perley et al. (2008b); Pro07: Prochaska et al. (2007); Cov08: Covino et al. (2008a); Pro08: Bea08: Beardmore et al. (2008), PeB08: Perley & Bloom (2008a); Prochaska et al. (2008); Vre08: Vreeswijk et al. (2008); Blo08: Bloom et al. (2008).

with ν in keV. Again for simplicity we assume that any cut-off frequency, at high as well as at low energies, is outside the IR–optical/X–ray frequency range.

The temporal parameters, described by the flat and steep decay indices, α_{fl} and α_{st} respectively, and the time T_A at which the two behaviours join, are assumed to be described by a smooth broken power-law:

$$L_L(\nu, t) = L_L(\nu, T_A) \frac{(t/T_A)^{-\alpha_{\text{fl}}}}{1 + (t/T_A)^{\alpha_{\text{st}} - \alpha_{\text{fl}}}}. \quad (5)$$

To summarise, the free parameters reproducing the late prompt emission are:

- (i) β_X — the spectral index of the late prompt emission in X-rays;
- (ii) β_o — the spectral index of the late prompt emission in the IR–optical;
- (iii) ν_b — the break frequency between the optical and the X-rays;

- (iv) $L_{\text{LX}}(T_{\text{A}})$ — the 0.3–10 keV luminosity of the late prompt emission at the time T_{A} ;
- (v) α_{fl} — the decay index for the shallow phase, before T_{A}
- (vi) α_{st} — the decay index for the steep phase, after T_{A} ;
- (vii) T_{A} — the time when the shallow phase ends.

These are 7 free parameters. It is worth stressing that, despite of their number, these are rather well constrained by observations. When the late prompt emission dominates, α_{fl} , α_{st} , T_{A} can be directly determined as well as one spectral index (usually β_{X} , since the late prompt emission is usually dominating in the X-ray range). Some degeneracy is present between ν_{b} and β_{o} , both of which control the importance of the optical flux due to the late prompt component: the same optical flux can for instance be reproduced assuming a steeper (flatter) β_{o} and a larger (smaller) ν_{b} , as the ratio between the 0.3–10 keV X-ray luminosity and the $\nu_{\text{o}}L(\nu_{\text{o}})$ optical luminosity of the late prompt is proportional to $\nu_{\text{b}}^{\beta_{\text{X}}-\beta_{\text{o}}}$.

3.3 Caveats

As our treatment is necessarily simplified, simply parametrising the late prompt emission, we analyse below the most important (or drastic) assumptions, trying to outline their effects.

- The afterglow calculations are based on the prescriptions by Panaitescu & Kumar (2000). In their analytical treatment the curvature of the emitting shell is neglected. The inclusion of the time delay between the emission times of photons received at any observer time would smooth out any relatively sharp feature of the light curve (especially when the injection or cooling frequency crosses the considered band). However the derived light curves are sufficiently accurate for the purposes of the present work.

- Almost all of the calculations of the afterglow light curves assume that ϵ_{e} and ϵ_{B} are constant in time. This is likely to be just a rough approximation, since the physical conditions at the shock front change in time (Γ as well as the density measured in the co-moving frame do change). As such a temporal dependence is not known or predicted, we are forced to adopt this simplification.

- The afterglow emission is assumed to be isotropic, *therefore no jet breaks* can be reproduced in the calculated light curves.

- The spectrum of the late prompt emission is assumed to be constant in time, in the observer frame. This is likely to be the most critical approximation, adopted just to minimise the number of free parameters. One might speculate that if this component originate by shells with decreasing bulk Lorentz factor (as in the models by Uhm & Beloborodov 2007, Genet, Daigne & Mochkovitch 2007 and Ghisellini et al. 2007), then it is likely that the observed break frequency ν_{b} would also decrease in time (if constant in the co-moving frame). While this would not affect the X-ray light curves (if ν_{b} is below the X-ray window even at early times), the optical emission would become relatively more important as time goes on. For instance, a plateau in the X-rays could correspond to a rising optical light curve. This suggests a possible observational test. Assume to select a burst in which both the optical and the X-ray light curves are dominated by the late prompt emission. If ν_{b} decreases in time, we should see two effects. First, the optical plateau should be shallower than the X-ray one (since the X-ray to optical flux ratio decreases as $\nu_{\text{b}}^{\beta_{\text{X}}-\beta_{\text{o}}}$). Secondly, when ν_{b} crosses the optical band, we should see a spectral steepening, since the decreasing ν_{b} acts as a cooling break. After ν_{b} has crossed the optical band, the optical and the X-ray fluxes should lie on the same power-law.

- The low and high frequency cut-offs of both the afterglow and late prompt emission have been neglected as free parameters. The

late emission spectrum might have a high frequency cut-off in the X-ray band. Given the current status of the X-ray observations, that do not detect such a cut-off, this simplification is reasonable.

- The late prompt emission is assumed to last forever, while, of course, it will die away after some time. This may happen, however, at very late times, when any X-ray or optical observations are not any longer feasible or when the GRB emission cannot be detectable (in the optical, emission can be dominated by the host galaxy or sometimes by a supernova associated to the burst).

- Flares, re-brightenings and/or bumps in the light curve are not accounted for. In our scenario, these are separated components, though in practice, their presence makes the choice of what data points to “fit” a bit subjective.

A final remark. Due to the above caveats, the values of the parameters for a single source may be subject to rather large uncertainties. In this sense the *distributions* of parameter values are much more meaningful. We could badly model an individual source, but the general conclusions could be right, if some coherence is found for the parameters of the entire sample.

4 RESULTS

Figs. 1–9 show the X-ray and optical light curves of the 33 GRBs together with the results of the modelling: dotted lines refer to the late prompt emission, dashed ones to the afterglow component and the solid lines to their sum.

The parameters inferred from the modelling of the light curves are reported in Table 2, together with a tentative classification of the bursts according to the dominant contribution: “A” stands for afterglow, “L” for late prompt, and “X” and “O” refer for X-ray and optical, respectively. For instance, XL–OA indicate that the X-ray flux is dominated by the late prompt, and the optical by the afterglow. When both type of emissions are comparable we use “M”, for mix. This also comprises the case when one component dominates in one time interval, and the other in another time interval. The number of bursts which can be described within these categories is summarised in Table 4. The X-ray flux is dominated by the late prompt emission or a mixture of late prompt and afterglow for the majority of GRBs, the opposite being true for the optical emission. Out of our 33 events, the most common cases are XM–OA (10 GRBs, namely a mix in the X-rays and afterglow in the optical) and XL–OM (8 GRBs, namely late prompt in the X-rays and a mix in the optical).

The overall result is that both components have comparable relevance in most cases. This is can be seen as a direct consequence of the different slopes of the light curves: since the late prompt emission is flatter than the afterglow up to T_{A} , and often steeper after this time, it is likely that the late prompt emission dominates or contributes around T_{A} even in the optical. Conversely, the afterglow may dominate or be important at very early and very late times (if there is no jet break). In other words the similar contribution of both components is the cause of the complex X-ray–optical behaviour observed.

4.1 Distribution of parameters

Figs. 10 and 11 show the distribution of all our input parameters. For comparison, in these figures we report the values found by

GRB	$E_{0,53}$	Γ_0	n_0	ϵ_e	ϵ_B	p	ν_b	β_X	β_o	α_{fl}	α_{st}	T_A	L_A	Class
1	2	3	4	5	6	7	8	9	10	11	12	13	14	15
050318	10	100	2	1.e-2	2.2e-4	2.5	1.e16	1.1	0.0	0.0	2.0	2.e3	434	XM-OA
050319	0.5	300	1.e-8	1.e-2	1.e-4	2.	1.e15	0.75	0.6	0.2	1.6	7.e3	623	XL-OM; XA early
050401	1.2	350	10	1.e-4	1.e-2	1.65	7.e16	0.9	-0.1	0.6	1.8	1.75e3	3.7e3	XM-OA
050408	2	200	3	1.e-3	3.e-2	2.8	6.e16	1.1	0.28	0.0	1.2	7.e3	133	XL-OM
050416A	0.6	200	3	1.e-4	8.e-5	1.67	7.e16	1.1	0.4	0.0	1.8	2.e3	17	XA-OA
050525A	1	100	1.e-8	1.e-3	2.e-2	2.3	5.e15	1.1	0.0	0.0	1.65	2.e3	133	XL-OA; XA early
050730	5	300	8	5.e-3	7.e-4	2.3	4.e16	0.9	0.15	0.2	2.6	2.5e3	1.3e4	XL-OM; XA late
050801	0.2	100	1.e-8	1.5e-2	7.e-4	2.4	2.e16	0.9	0.1	0.0	1.5	1.e3	112	XL-OA; XA early
050802	3	200	3	2.e-2	2.e-4	2.3	1.e16	1.1	0.0	0.0	1.8	1.5e3	667	XM-OA
050820A	4	120	10	1.e-3	1.e-2	1.85	5.e16	1.1	0.0	-0.2	1.6	2.5e3	5.e3	XM-OA
050824	0.7	100	1	2.e-4	3.e-3	1.75	1.e16	1.1	0.0	0.0	1.2	1.e4	3.33	XA-OA
050922C	10	250	2	2.e-3	1.2e-3	2.4	2.e16	1.1	0.5	0.0	1.5	8.e2	1334	XL-OM; XA early
051111	5	120	5.e-9	1.e-3	1.e-3	2.1	2.e15	1.1	0.5	-0.1	1.5	5.e2	1.e3	XM-OM
060124	5	110	3	5.e-3	6.e-4	2.	2.e16	1.1	0.1	0.2	1.6	9.e3	1.7e3	XL-OM; XA early
060206	4	180	2	5.e-2	6.e-4	2.6	4.e16	1.1	0.1	-0.3	1.5	2.5e3	5.e3	XL-OM
060210	80	100	1.e-8	5.e-3	8.e-4	2.15	1.5e16	1.25	1.25	0.0	1.7	2.8e2	3.1e4	XA-OL
060418	5	200	10	1.e-3	1.e-2	2.3	2.e16	1.1	0.1	0.1	1.6	2.8e2	4.3e3	XL-OA
060512	3	200	10	1.2d-4	1.e-3	2.15	1.e15	1.1	0.5	0.0	1.3	8.e2	3.33	XA-OA
060526	4	300	10	3.e-4	6.e-3	1.9	8.e15	1.1	0.6	0.0	1.9	6.e3	167	XM-OM
060614	0.03	100	1	2.e-3	2.e-5	2.	5.e16	1.1	0.6	-0.5	2.1	4.5e4	0.5	XL-OL; XA-OA early
060729	0.5	110	3	4.e-3	1.e-3	2.3	2.e15	1.1	0.5	-0.1	1.4	3.5e4	50	XL-OL; XA-OA early
060904B	0.3	100	3	2.8e-2	4.e-4	2.15	2.e16	1.1	0.0	0.5	1.6	1.3e3	100	XM-OA; OL early
060908	1	400	10	2.e-3	3.e-3	2.3	6.e15	1.1	0.4	0.3	1.5	3.e2	500	XM-OA
060927	8	220	30	3.e-3	1.e-4	2.3	3.e16	1.1	0.0	0.0	1.7	4.e2	2.7e3	XM-OA
061007	60	200	1.e-8	3.e-3	3.e-4	2.6	8.e15	1.1	0.0	0.0	1.75	5.e1	3.e5	XM-OA
061121	6	110	3	4.e-4	1.e-2	2.	2.e16	1.1	0.0	0.0	1.65	1.5e3	1.e3	XM-OA
061126	3	100	1.e-8	1.e-3	2.e-4	2.5	1.e16	1.1	0.0	0.0	1.45	3.e3	300	XL-OM
070110	3	100	1	5.e-4	6.e-3	1.8	5.e16	1.1	0.0	0.0	1.7	1.e3	1.e3	XA-OA
070125	4	300	1	1.3e-2	6.e-2	2.65	1.e15	1.6	1.6	-0.4	2.2	5.e4	0.3	XA-OM
071003	4	100	1.e-8	1.e-3	1.5d-4	2.3	1.e16	1.1	0.8	-0.7	1.7	1.5e4	50	XL-OM; XA early
071010A	5	120	3	3.e-4	6.e-3	2.	5.e15	1.1	0.0	-0.3	1.4	2.e4	17	XL-OA; XA early
080310	1	120	6	1.e-3	7.e-3	1.95	1.e16	1.1	0.4	-0.5	1.7	1.3e3	1.3e3	XM-OA; OM mid
080319B	50	400	10	1.e-3	8.e-4	2.7	6.e16	1.1	-0.1	0.0	1.65	4.e1	1.3e6	XL-OA

Table 2. Input parameters for the afterglow component (columns 2–7) and for the late prompt emission (columns 8–14). Col 1: Burst Id; Col 2: Fireball kinetic energy (after the early prompt emission, in units of 10^{53} erg); Col 3: Initial bulk Lorentz factor; Col 4: density of circum–burst medium: values equal or larger than 1 are for a homogeneous density; values much smaller than 1 correspond to a wind like profile; the listed value is \dot{M}_w/v_w , where \dot{M}_w is the mass loss rate in M_\odot/yr and v_w is the wind velocity in km s^{-1} . Col. 5 and 6: equipartition parameters ϵ_e and ϵ_B ; Col 7: slope of the assumed relativistic electron distribution; Col. 8: spectral break of the late prompt emission (in Hz); Col. 9 and 10: high and low energy spectral indices of the late prompt emission; Col. 11 and 12: decay slopes of the late prompt emission, before and after T_A listed in Col. 13 (in sec); Col. 14: luminosity (in units of 10^{45} erg s^{-1}) in the 0.3–10 keV energy range of the late prompt emission, at the time T_A ; Col. 15: Burst classification (see text).

Panaitescu & Kumar (2002) for 10 pre–Swift bursts³ This is to be expected, since in our interpretation the X–ray luminosity in the majority of cases is not produced by the afterglow, which is thus less energetic.

Most (25 out of 33) afterglows can be consistently described by the interaction of the fireball with a homogeneous medium. This

³ Panaitescu & Kumar (2002) give the collimation corrected value for the isotropic kinetic energy of the fireball after the early prompt phase. We have then divided this value by $(1 - \cos \theta_j)$ to get the isotropically equivalent value of E_0 to be compared with the values found for our bursts. Note that Γ_0 does not affect the properties of the afterglow after its onset, and is therefore not an important parameter for Panaitescu & Kumar (2002), who are fitting data taken much later than the afterglow onset (with the exception of GRB 990123). The afterglow parameters found for our bursts are rather standard, being similar to the ones obtained by Panaitescu & Kumar (2002) (see also Panaitescu & Kumar 2001a and 2001b). The distribution of the circum–burst density n_0 is narrower for the bursts in our sample, while the distributions of ϵ_e and ϵ_B are centred on smaller values.

is especially the case when the optical light curve indicate the onset of the afterglow itself (i.e. a very early rising phase), that cannot be reproduced with a wind–like density profile. The latter in fact produces almost flat optical light curves in the early phases. The homogeneous densities are very narrowly distributed around a mean value of $\langle n_0 \rangle \sim 3 \text{ cm}^{-3}$. For 8 GRBs (see Tab. 2) a better modelling can be achieved invoking a wind–like density profile. All but one of these 8 bursts can be modelled with a value of the ratio of the mass loss rate and the wind velocity of $\dot{M}_w/v_w = 10^{-8} (M_\odot \text{ yr}^{-1})/(\text{km s}^{-1})$ that can correspond to $\dot{M}_w = 10^{-5} M_\odot \text{ yr}^{-1}$ and $v_w = 10^3 \text{ km s}^{-1}$. The remaining burst require half of this value. Similarly to what had been found by Panaitescu & Kumar (2002) the afterglow parameters distribution are quite broad, i.e. they do not cluster around typical values. Exceptions are the density n_0 and the bulk Lorentz factor Γ_0 .

Also the distributions of some late prompt parameters (i.e. T_A , L_{T_A} and ν_b) are rather broad, while β_o and the temporal slopes α_{fl} and α_{st} are more narrowly distributed. The values of T_A range from

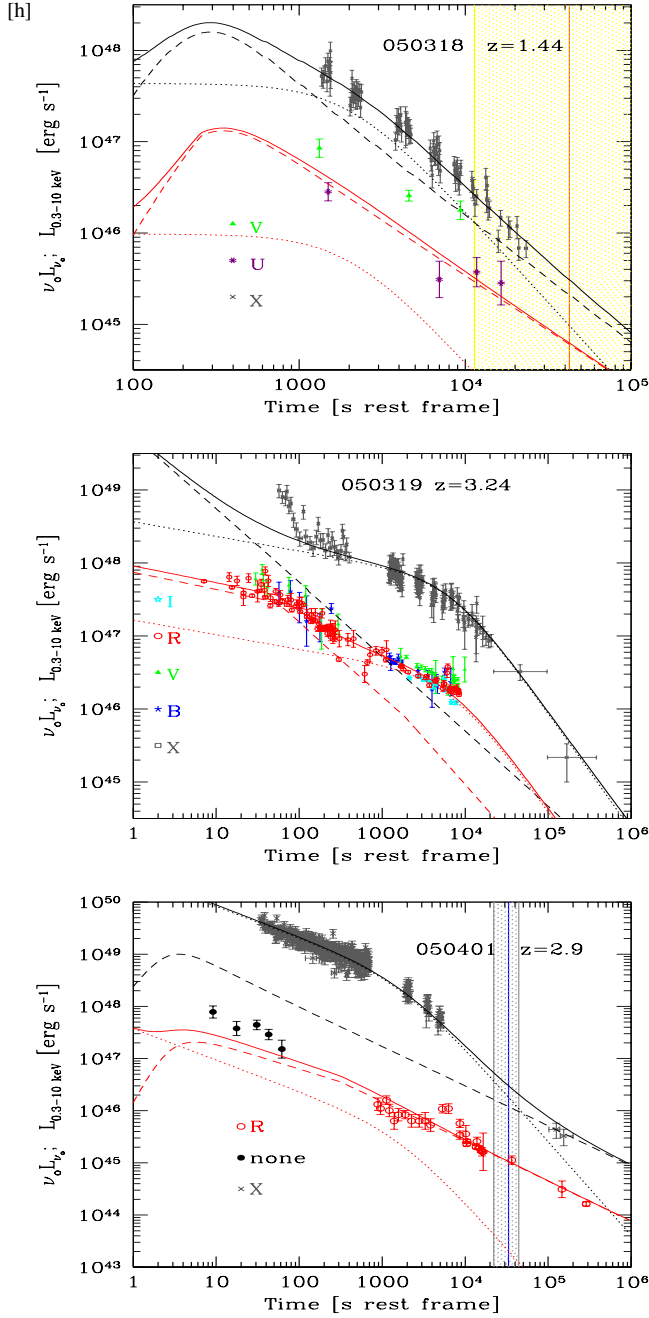


Figure 1. Figs 1-9. X-ray (in grey) and optical (different symbols, as labelled) light curves. Lines indicate the model fitting: afterglow (dashed), late prompt (dotted) and their sum (solid). Black lines refer to the X-rays, light grey (red in the electronic version) for the optical. The vertical line (and shaded band) correspond to the rest frame jet break times (and their 3σ uncertainty). Grey lines and stripes correspond to jet break times as reported in the literature (references are listed in Ghirlanda et al. 2007), light grey (yellow in the electronic version) lines and stripes refer to jet times expected if the burst followed the Ghirlanda relation. These are shown only for bursts with measured E_{peak} , the peak energy of the prompt emission. References for the optical data can be found in the appendix.

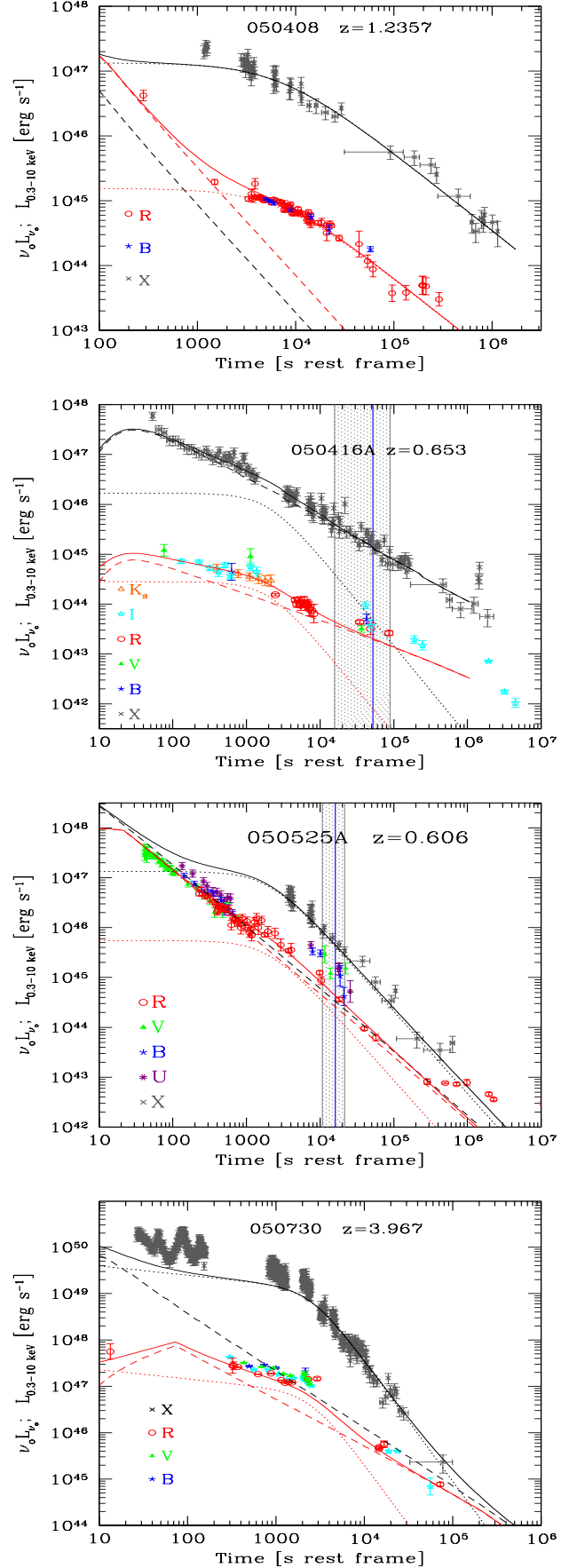


Figure 2. Same as in Fig. 1.

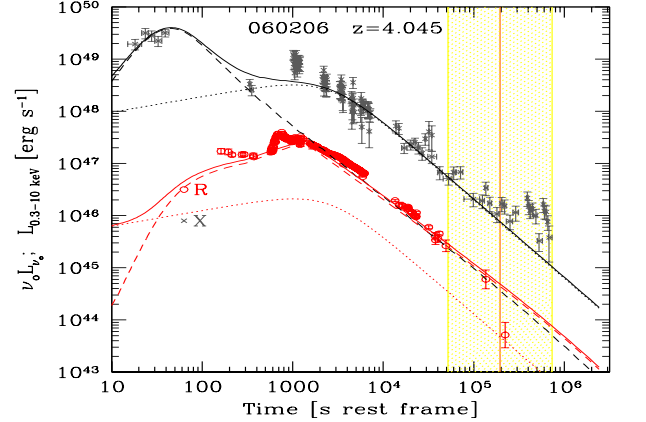
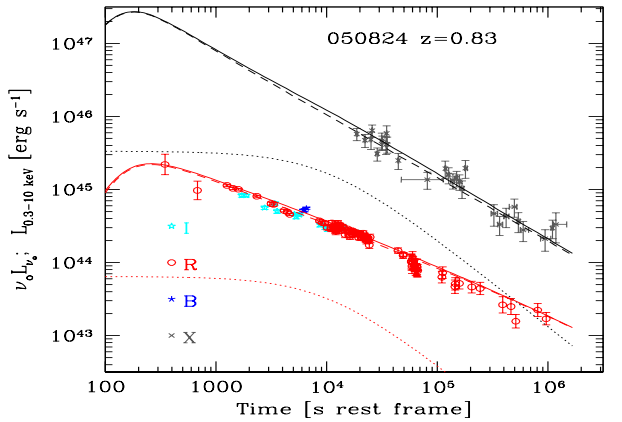
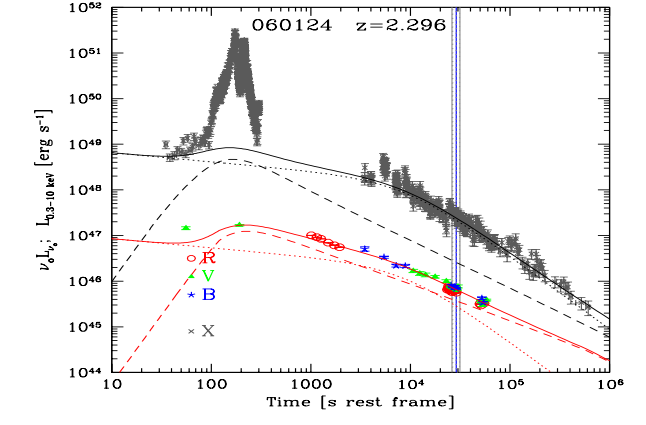
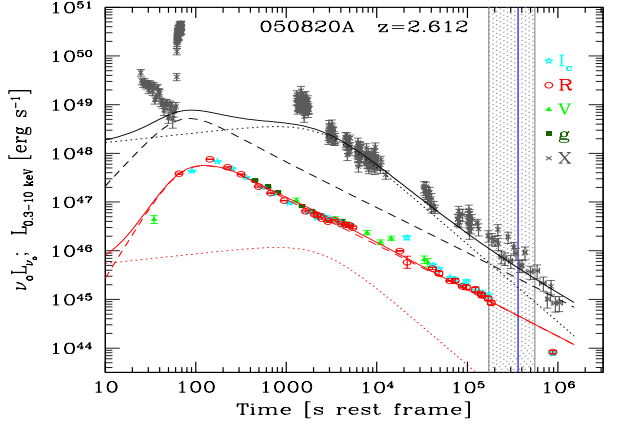
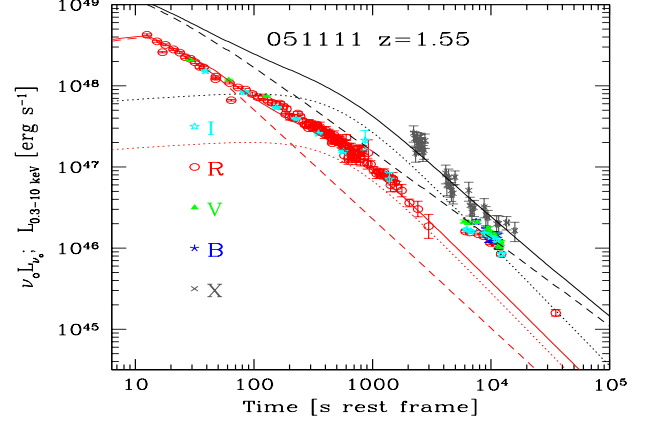
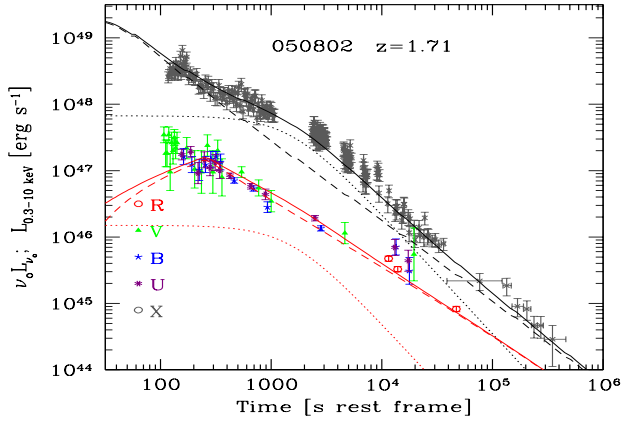
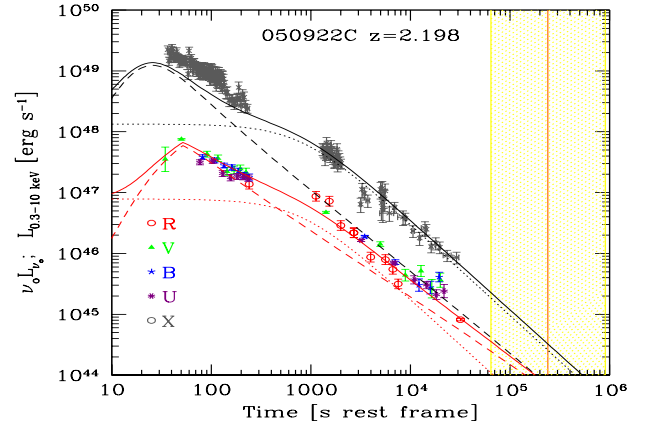
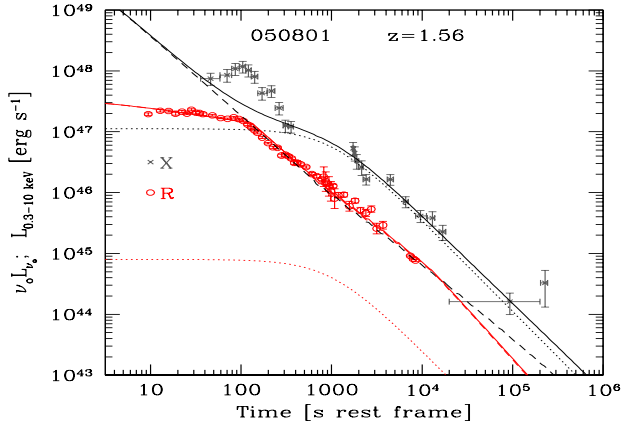


Figure 3. Same as in Fig. 1.

Figure 4. Same as in Fig. 1.

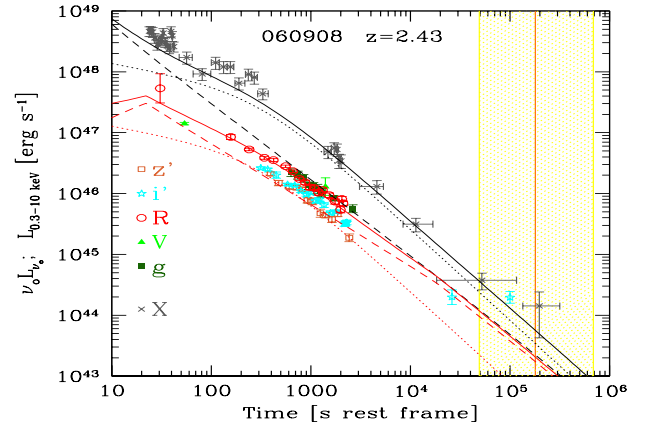
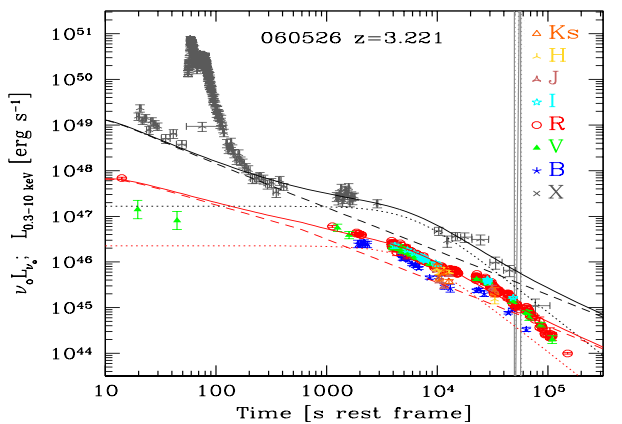
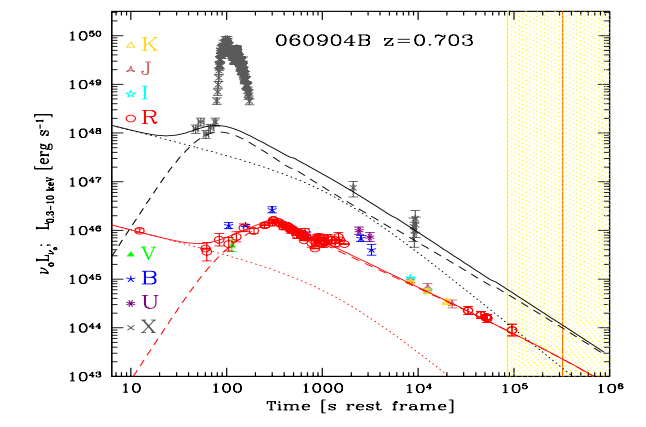
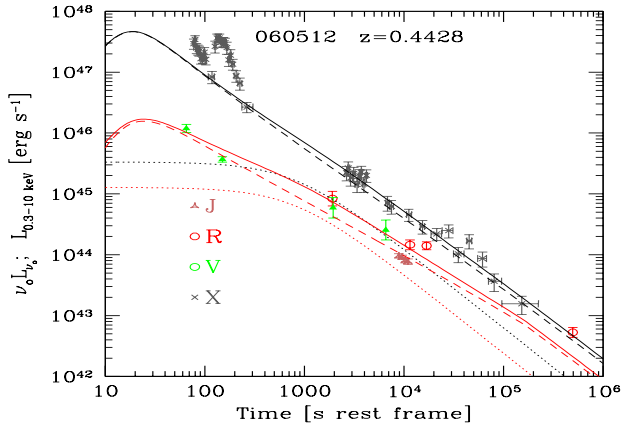
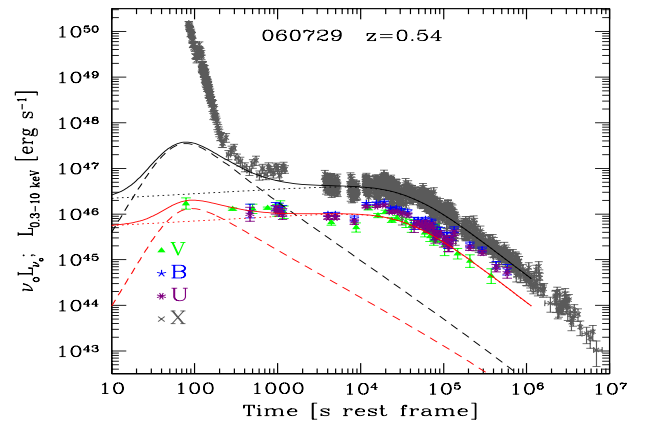
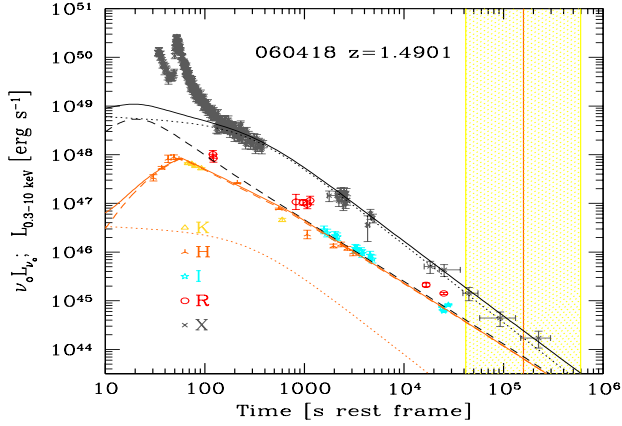
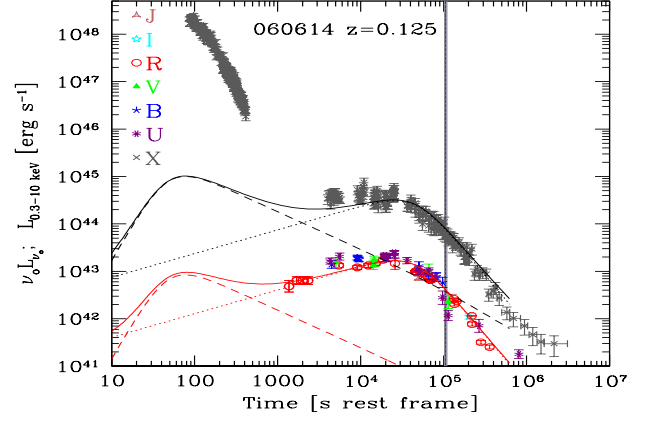
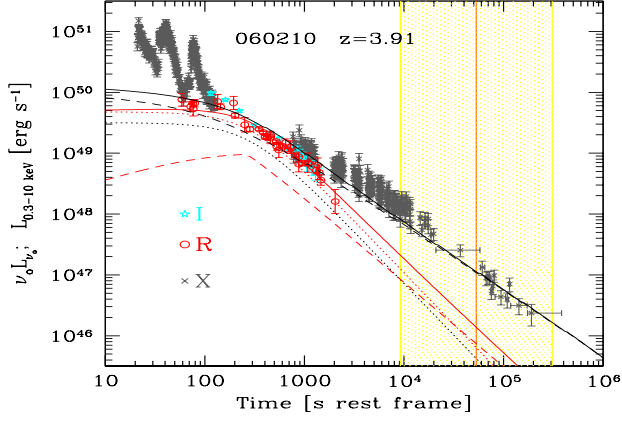


Figure 5. Same as in Fig. 1.

Figure 6. Same as in Fig. 1.

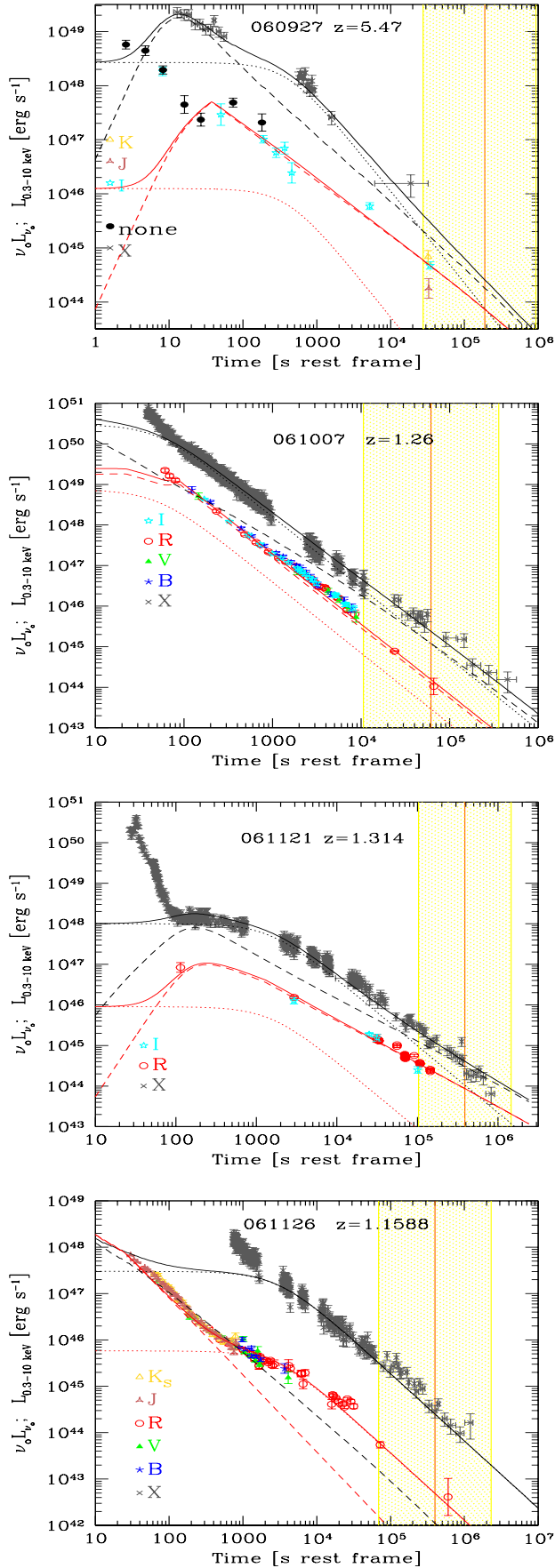


Figure 7. Same as in Fig. 1.

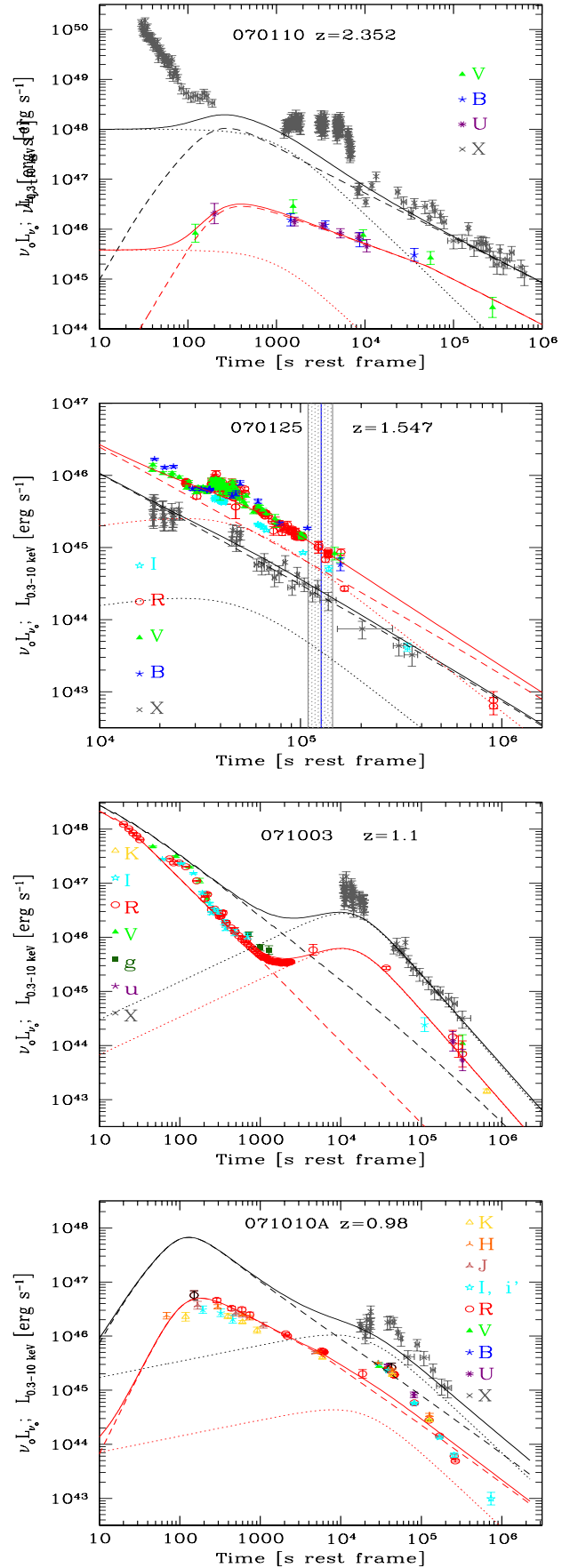


Figure 8. Same as in Fig. 1.

XL	15	
XA	6	
XM	12	
OL	3	
OA	19	
OM	11	
XL-OL	2	both with XA-OA very early
XA-OA	4	
XM-OM	2	
XL-OA	5	3 bursts with XA early
XA-OL	1	
XM-OL	0	
XM-OA	10	1 with OL early, one with OM mid
XA-OM	1	
XL-OM	8	4 with XA early, 1 with XA very late

Table 3. Number of sources dominated by different components: XA (OA): X-ray and optical flux dominated by the Afterglow emission; XL (OL): X-ray and optical flux dominated by the late prompt emission; XM (OM): X-ray and optical fluxes where the late prompt and afterglow emission are relevant.

10^2 to 10^4 s or more (in the rest frame), and are (anti-)correlated with the late prompt luminosity at T_A , as shown in Fig. 12. This confirms the correlation found by Dainotti, Cardone & Capozziello (2008). This results in a narrow distribution of $T_A L_{T_A}$ (Fig. 11).

The distributions of β_0 and ν_b must be taken with caution, since the model fixes only their combination, and only in a few GRBs they can be constrained separately (i.e. when the optical light curve is dominated by the late prompt emission and the spectral index during this phase is known).

The distribution of α_{st} is intriguing, since it is centred around a mean value of 1.6. This is very close to $5/3$, the predicted decay of the accretion rate of fall-back material (see also §5 where this point is discussed in more depth). The values of α_{fl} cluster around 0.

In Fig. 11 we show the distribution of $T_A L_{T_A}$, and in Fig. 13 we show $T_A L_{T_A}$ as a function of E_{iso} . The two quantities are correlated (albeit poorly) and the energy contained in the late prompt emission (of which $T_A L_{T_A}$ is a proxy) is at most comparable with E_{iso} . More frequently $T_A L_{T_A}$ is one or two orders of magnitude smaller than E_{iso} , in agreement with the findings by Willingale et al. (2007).

Fig. 11 shows also the distribution of $E_{iso}/[E_0 + E_{iso}]$. This ratio represents η , the fraction of the total energy of the fireball required to produce the observed early prompt radiation. In Fig. 14 this fraction is shown as a function of E_{iso} . Although there is a weak positive correlation, the mean value is well defined and corresponds to $\eta \sim 0.1$.

4.2 Jet breaks

A currently hot debate concerns the absence of jet breaks in the light curves of GRB afterglows. In the scenario we propose the light curve comprises two components of which only the afterglow one should present a jet break (at t_j). It follows that jet breaks should be more often detectable in the optical, rather than being achromatic, and the after-break slopes may be shallower than predicted by the closure relations.

No jet breaks — When the flux is dominated by the late prompt emission in both the optical and the X-ray bands, jet breaks may

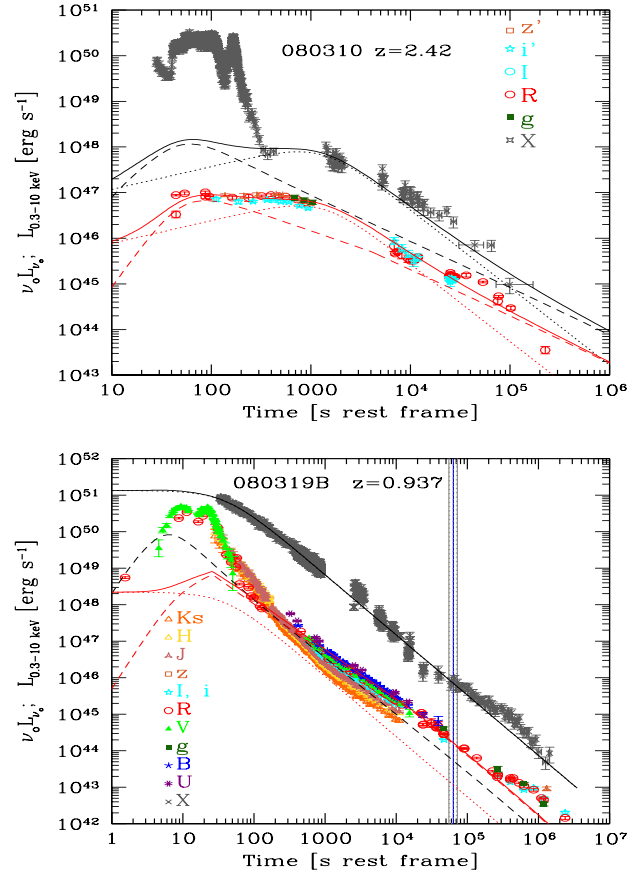


Figure 9. same as in Fig. 1.

become unobservable. The late prompt emission (at least after a few thousand seconds) does so for 6 GRBs of the sample (namely GRB 050319, GRB 050408, GRB 060614, GRB 060729, GRB 061126 and GRB 071003). Therefore, for these bursts, no jet break is predicted to be visible if the late prompt light curve continues unbroken for a long time – if the late prompt component instead breaks, we might erroneously interpret this as a jet break.

Achromatic jet breaks — Viceversa, an achromatic jet break should be observed when both in the optical and X-ray light curves the afterglow emission prevails, at least when the jet break is likely to occur. 16 GRBs of the sample could show such an achromatic break (GRB 050318, GRB 050401, GRB 050416A, GRB 050802, GRB 050820A, GRB 050824, GRB 060512, GRB 060904B, GRB 060908, GRB 060927, GRB 061121, GRB 070110, GRB 070125, GRB 071010A, GRB 080310, GRB 080319B). Emission in several of these bursts – although dominated by afterglow emission, especially in the X-ray band, at late times – still comprises a relevant contribution from the late prompt component. Therefore the steepening of their light curve after t_j should be shallower than what the standard afterglow theory predicts.

Chromatic jet breaks — When the late prompt is dominating in one band, and the afterglow in the other, a jet break should be visible only in the afterglow-dominated band. According to our findings a jet break could be present in the optical but not in the X-rays band in 9 GRBs (GRB 050525A, GRB 050730, GRB 050801, GRB 050922C, GRB 060124, GRB 060206, GRB 060418, GRB 060526 and GRB 061007). Instead, 2 GRBs (GRB 051111 and GRB 060210), could show a jet break in X-rays but not in the optical.

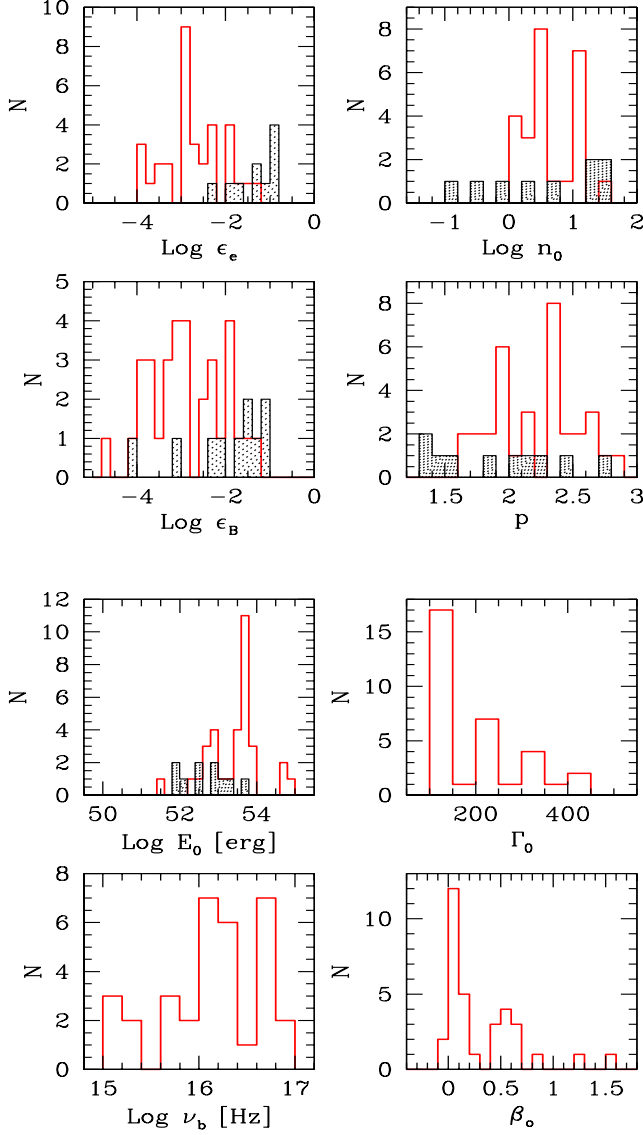


Figure 10. Top 4 panels: distribution of the values of the micro-physical parameters ϵ_e , ϵ_B , homogeneous density n_0 , and electron slope p . Bottom 4 panels: distribution of the isotropically equivalent initial kinetic energy E_0 , bulk Lorentz factor Γ_0 , break frequency ν_b and optical spectral index for the late prompt emission β_o . The hatched areas correspond to the distribution of parameters found by Panaitescu & Kumar (2002) fitting the afterglow of 10 pre-Swift bursts. They are shown for comparison.

In Figs. 1–9 we indicate the time at which a jet break has been reported to be detected or the time at which a jet break is expected to be seen if the burst were to follow the $E_{\text{peak}} - E_\gamma$ (Ghirlanda) relation (Ghirlanda, Ghisellini & Lazzati 2004, updated in Ghirlanda et al. 2007) (see the figure caption). The latter ones are estimated only for bursts with measured E_{peak} , the peak energy of the νF_ν spectrum of the proper prompt emission. We found no contradictory cases (i.e. an observed jet break occurring in a late prompt-dominated GRB), except for GRB 060614.

There are some additional bursts for which the presence of a jet break has been claimed in the literature. For instance, in GRB 050319 Cusumano et al. (2006) suggest that the break in the X-ray light curve at 27,000 s (observed time) could be a jet break, but also discuss the problems with this interpretation due to the

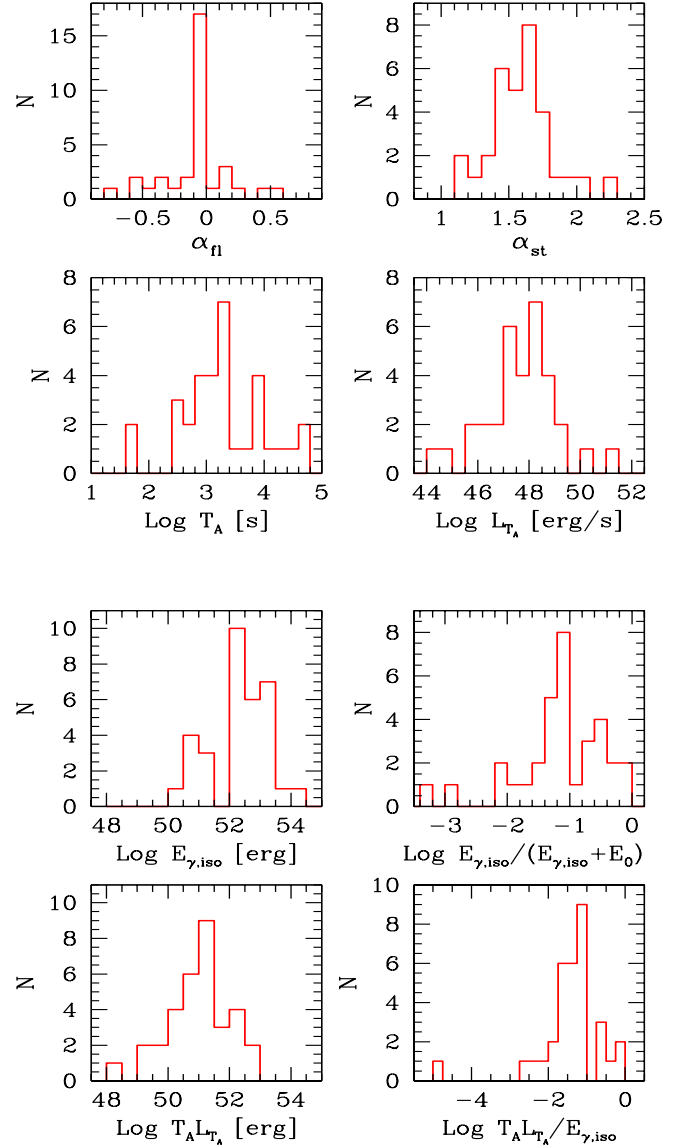


Figure 11. Top 4 panels: distributions of the decay indices of the late prompt emission, α_{II} and α_{st} , of T_A and of the 0.3–10 keV luminosity at the time T_A . Bottom 4 panels: distributions of the isotropic energy $E_{\gamma,\text{iso}}$ of the early prompt radiation, of the ratio $E_{\gamma,\text{iso}}/(E_{\gamma,\text{iso}} + E_0)$, which provides an estimate of the efficiency of the prompt emission; of the energy $T_A L_{T_A}$, and of the ratio $T_A L_{T_A}/E_{\gamma,\text{iso}}$.

unusual pre- and post-break slopes. In our scheme, the observed break simply corresponds to T_A .

For GRB 050730, Pandey et al. (2006) consider the change of slopes at ~ 0.1 d (observed time) in the optical light curve as indicative of a jet break. In our interpretation, instead, the change of the flux decay slope is due to the late prompt emission providing a relevant contribution after $\sim 3 \times 10^3$ (rest frame time).

Malesani et al. (2007) claim the presence of a possible jet break in the optical light curve of GRB 070110, at ~ 5 days (observed time). According to our findings, this can indeed be a jet break that should also be visible in X-rays.

In the light curves examined here, there are also a few examples of slope changes that could be jet breaks, but for which we could not find any report in the literature. The optical light curve of

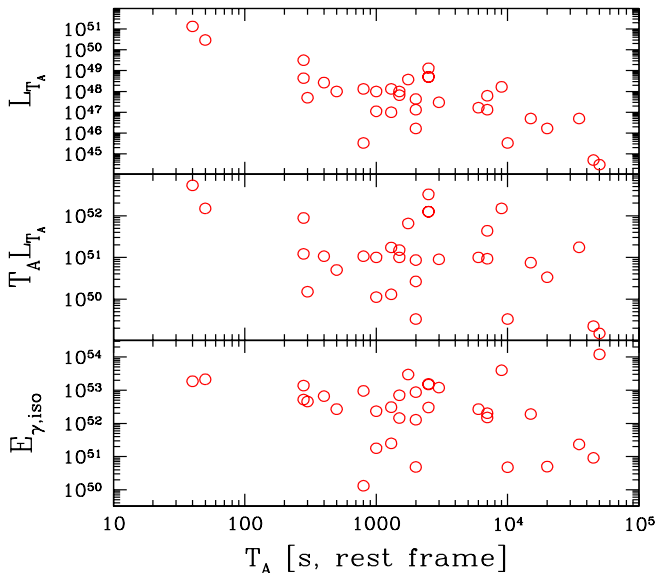


Figure 12. The luminosity of the late prompt emission L_{T_A} (in erg s^{-1}) at T_A , the corresponding energy $T_A L_{T_A}$ (in erg) and the isotropic energy $E_{\gamma,\text{iso}}$ (in erg) as functions of T_A . Note that L_{T_A} anti-correlates with T_A , in such a way that the energy $T_A L_{T_A}$ has a relatively narrow distribution (see also the corresponding histogram in Fig. 11).

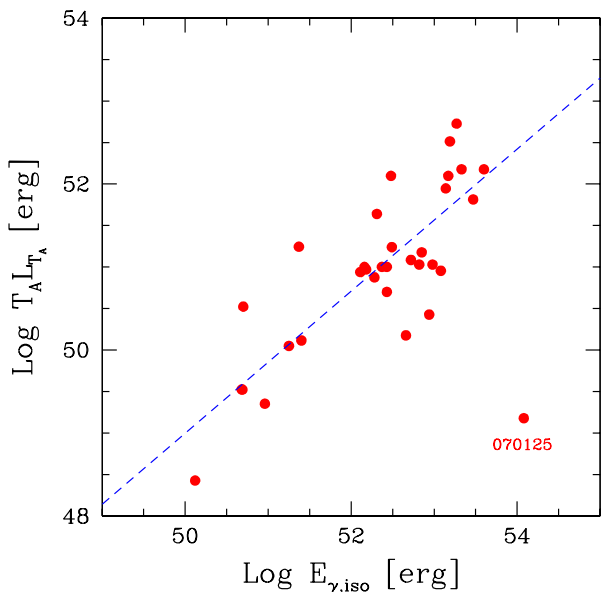


Figure 13. Energy of the late prompt emission, estimated as $T_A L_{T_A}$, as a function of the isotropic energy of the prompt emission, $E_{\gamma,\text{iso}}$. The dashed line corresponds to the least square fit, $[T_A L_{T_A}] \propto E_{\gamma,\text{iso}}^{0.86}$ (chance probability $P = 2 \times 10^{-7}$, excluding the outlier GRB 070125).

GRB 060206 may be one of such cases (see the last optical point in Fig. 4). For this GRB the presence of the jet break is expected only in the optical, since the X-rays are dominated by the late prompt component. Note that the corresponding t_j would make this burst consistent with the Ghirlanda relation (see the vertical grey line in Fig. 4). Another example is visible in the X-ray flux decay of GRB 061121, at $\sim 10^5$ s (rest frame, see Fig. 7). Unfortunately, there are no optical data at this late time to confirm it. Again, if this is a

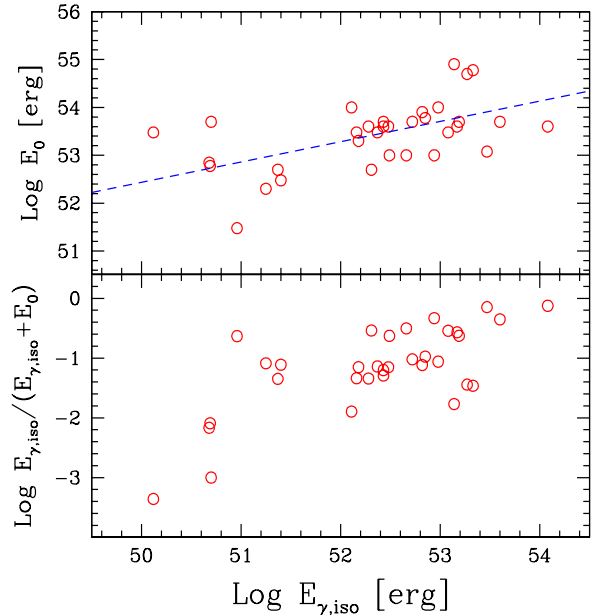


Figure 14. Top panel: the kinetic energy E_0 after the prompt emission as a function of $E_{\gamma,\text{iso}}$. The dashed line is a least square fit, yielding $E_0 \propto E_{\gamma,\text{iso}}^{0.42}$ (chance probability $P \sim 10^{-3}$, excluding GRB 070125). Bottom panel: the efficiency of the prompt emission estimated as $E_{\gamma,\text{iso}}/(E_{\gamma,\text{iso}} + E_0)$ as a function of $E_{\gamma,\text{iso}}$. There seems to be weak correlation, in the sense that weaker bursts would have the smaller efficiency. See the corresponding distribution in Fig. 11. Here and in the other figures, the plotted values of $E_{\gamma,\text{iso}}$ are neither bolometric nor K-corrected, but refer to the observed 15–150 keV range.

jet break, the burst would be consistent with the Ghirlanda relation (see the vertical grey line in Fig. 7). Also in GRB 071010 there could be a jet break in optical, after $\sim 10^5$ s (rest frame, see Fig. 8) but its interpretation is difficult because of an optical/X-ray flare occurring just before. Finally, for GRB 080310, a steepening of the optical light curve after $\sim 10^5$ s (rest frame, see Fig. 9) could be a jet break, as also supported by a steepening also in the X-ray light curve, that is (marginally) dominated by the afterglow component.

We plan to discuss in more detail these possible jet breaks in a forthcoming paper (Nardini et al., in preparation).

4.3 Prompt and afterglow energetics

As the X-ray luminosity L_X is found to be often dominated by the late prompt emission, *it does not provide a proxy for the afterglow bolometric luminosity*. Since L_X exceeds what observed in the other spectral bands, the estimated luminosities and total energetics produced by the afterglow are radically smaller than what simply inferred from L_X .

This exacerbates the problem of understanding why the early prompt emission is larger than the afterglow one, if the former is dissipated in internal shocks. In fact, while in external shocks, believed to be responsible for the afterglow, a fraction of the whole fireball kinetic energy is available, in internal shocks only a fraction of the *relative* kinetic energy between two colliding shells can be dissipated as radiation. If such fractions are similar, the “bolometric afterglow fluence” is expected to be a factor ~ 10 larger than the bolometric early prompt fluence. The opposite is observed, and the discrepancy is more extreme if L_X provides only an upper limit to the afterglow contribution, as in our interpretation.

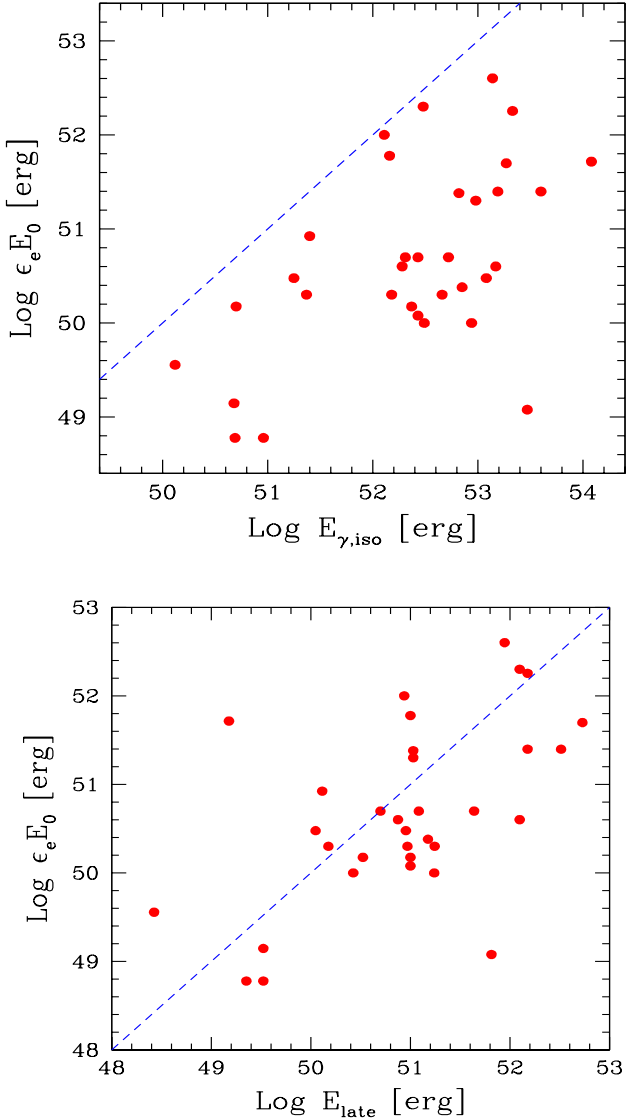


Figure 15. The energetics of the afterglow component, estimated as $\epsilon_e E_0$, as a function of: (top panel) $E_{\gamma, \text{iso}}$, the energetics of the prompt emission as measured in the 15–150 keV band (rest frame) (top panel) – the dashed line corresponds to equal values; (bottom panel) E_{late} , the energetics of the late prompt emission, as measured in the (rest frame) 0.3–10 keV band and approximated by $T_A L_{T_A}$.

Bearing in mind that it is often dangerous to claim correlations between luminosities or energetics, since both quantities are function of redshift, we can compare Fig. 12 with Fig. 13. It can be seen that the correlation between the late prompt energetics measured by $T_A L_{T_A}$ and $E_{\gamma, \text{iso}}$ is stronger than the correlation between the kinetic energy (after the early prompt) E_0 and $E_{\gamma, \text{iso}}$. A least square fit yields $[T_A L_{T_A}] \propto E_{\gamma, \text{iso}}^{0.86}$ (chance probability $P = 2 \times 10^{-7}$), and $E_0 \propto E_{\gamma, \text{iso}}^{0.42}$ (chance probability $P \sim 10^{-3}$). If the $T_A L_{T_A} - E_{\gamma, \text{iso}}$ relation is not a mere product of the common redshift dependence (which however should also affect the $E_0 - E_{\gamma, \text{iso}}$ relation) this suggests that the early and the late prompt phases of emission are related.

In Fig. 15 (top panel) $\epsilon_e E_0$ (which can be considered as an upper limit to the bolometric afterglow luminosity) is compared to $E_{\gamma, \text{iso}}$, the energetic of the prompt emission as measured in the 15–

150 keV band (rest frame). $E_{\gamma, \text{iso}}$ exceeds the afterglow energetics by almost two orders of magnitudes. In the bottom panel of the same figure $\epsilon_e E_0$ is plotted against the energetics of the late prompt emission E_{late} , approximated by the quantity $T_A L_{T_A}$. These quantities do not correlate, suggesting that they are two separated components.

To summarise: all indications gathered from the analysis of the energetics suggest that what we have called “late prompt emission” is a phenomenon not related to the afterglow, but it is more connected to the same engine producing the early prompt. Furthermore, the energetics associated to the afterglow emission is on average a small fraction of the total energy of the burst.

5 DISCUSSION AND CONCLUSIONS

The proposed scheme appears to be suitable to account for the diversity of the optical and X-ray light curves of GRBs, at the expense of introducing, besides the standard afterglow emission resulting from the external (forward) shock, another component. This has been simply parametrised with 7 free parameters. The distributions of these parameters are not particularly clustered around mean values, except for the time decay slopes α_{fl} and α_{st} (see below). However, this should not be taken as a potential problem for the proposed idea, since even the well established afterglow model, when applied to the optical and X-ray afterglows of pre-Swift GRBs, yield broad parameter distributions (see Fig. 10 and Panaitescu & Kumar 2002).

Our phenomenological approach should be considered as a first step towards the construction of a convincing physical model. As discussed in the introduction, there has been already a blooming of theoretical ideas, but a general consensus has not yet been reached. Our findings can shed some light and help to discriminate among the different proposals.

As an illustrative example, the proposed scenario can be contrasted with the alternative idea that GRBs are characterised by two jets with different opening angles (see the Introduction). In the latter interpretation, if the line of sight lies within the wide cone but outside the narrow one, the emission from the narrow jet will be observable when Γ has decreased to $\Gamma \sim 1/\theta_v$ and the corresponding afterglow light curve can reproduce the flat–steep–flat behaviour and present a break (at T_A). However, it is hard to explain why the flat–steep–flat trend is not observed in the optical, as in a (narrow jet) afterglow the optical and X-ray fluxes should temporally track each other. The “late prompt” scenario appears to provide a better interpretation of the data.

Within the proposed scheme, some light can be shed on the puzzling issue about jet breaks.

They can be achromatic if the afterglow component is observed in different bands. These may not be the case for several bursts. Furthermore, there are a few in which the late prompt emission, dominating both the optical and X-ray flux, hides jet breaks at all times. For these bursts a break at the time T_A is visible in both the X-ray and optical bands, and it can be erroneously be taken as a jet break, since it is achromatic. Only a densely sampled light curve in both bands can help to discriminate the presence of a real jet break. Note that the bursts in our sample, selected for having an estimate of extinction in the host, are better sampled optically than the rest of the bursts, for which it would be difficult to reliably estimate the relative importance of the two components.

Another relevant consequence of our scenario is that, even when a jet break is observed, the after-break light curve can be

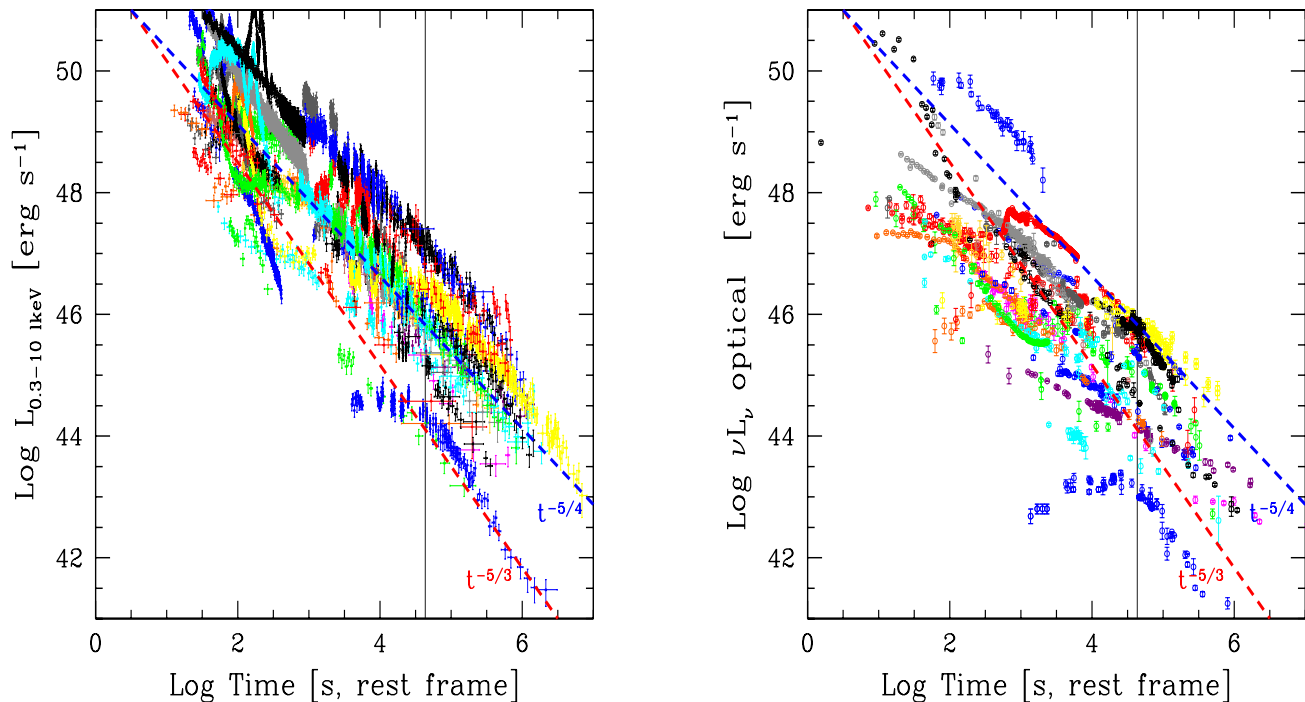


Figure 16. The light curves of all the 33 GRBs in the X-rays (left panel) and optical (right panel). For comparison, the dashed lines correspond to $t^{-5/4}$ and $t^{-5/3}$, as labelled. Especially in the X-rays, the luminosity profile seems to be flatter than $t^{-5/3}$ and closer to a $t^{-5/4}$ decay. However, this behaviour is due to the contribution in some GRBs of the afterglow emission at late times, flattening the overall light curve. See Fig. 17 for comparison.

flatter than predicted, since the late prompt flux can contribute after t_j . This implies that the so-called closure relations, linking the flux decay slopes before and after the break with the spectral index, should be taken with care. In this respect, it is worth stressing that the closure relations, and in general the simplified afterglow scenario predicting them, treat the micro-physical parameters ϵ_e and ϵ_B as constant in time. We adopt the same simplification, but this might become a crucial issue once we will have a convincing physical interpretation predicting their time behaviour.

From our modelling the steep decay of the late prompt emission can be described by a power-law with slope $\alpha_{st} \sim 1.6$. This is intriguingly similar to the time dependence of the mass accretion rate during the fall-back phase, and to the average decay of the X-ray flare luminosity, as analysed by Lazzati, Perna & Begelman (2008). This is *not* the average decay slope observed: the X-ray and optical light curves are flatter than $L(t) \propto t^{-5/3}$ (see Fig. 16), but this is due to the contribution, especially at early and late times, and in the X-rays, of the afterglow contribution. Fig. 17 shows the results of our light curve modelling for the optical and X-rays bands. The late prompt light curves are indeed steeper, on average, than the sum of the two components that reproduce the data. We consider this as a main result of our analysis, because it suggests that the late prompt emission can be interpreted as due to the late time accretion onto a black hole of fall-back mass, namely material that failed to reach the escape velocity from the exploding progenitor star, and falls-back. According to analytical results (Chevalier 1989) and numerical simulations (e.g. Zhang, Woosley & Heger 2008), the accretion rate decreases in time as $t^{-5/3}$, and can continue for weeks, enough to sustain late prompt emission

even at very late times. Our finding also agrees with that obtained by Lazzati, Perna & Begelman (2008) by analysing X-ray flares. They found that the average luminosity of X-ray flares, for a sample of GRBs with known redshift, also decays like $t^{-5/3}$. Such an agreement then suggests that both the X-ray flares and the late prompt emission have a common origin, related to the accretion of the fall-back material. It remains to be explained why this phase is observed after T_A that in some cases can be as long as 10^4 sec or more, while the simulations predict a quasi-constant accretion rate for 10^2 – 10^3 s (MacFadyen, Woosley & Heger 2001). There are at least two possibilities. The first one is suggested by the simulations of Zhang, Woosley & Heger (2008) (see their Fig. 2) which include the effect of the reverse shock running through the fall-back material. When the reverse shock reaches the inner base the material is slowed down, and thus the accretion rate is enhanced. The asymptotic $t^{-5/3}$ phase can thus be delayed. The second possibility has been suggested by Ghisellini et al. (2007): even if the total flux produced by the late prompt phase is decaying at the rate $t^{-5/3}$, a decreasing Γ implies that the observed emission comes from an increasing surface ($\propto 1/\Gamma^2$), making the observed decay flatter than $t^{-5/3}$, until, at T_A , $\Gamma \sim 1/\theta_j$. After T_A the whole emitting surface contributes to the detected flux, and the flux decreases as $t^{-5/3}$.

Fig. 17 shows that the sum of the late prompt and afterglow emission makes the optical fluxes to cluster. This occurs because the late prompt emission – though usually not dominant in the optical – narrows the distribution of the optical luminosities at a given time. The vertical dotted line in the figure corresponds to the time (12 hours) at which Nardini et al. (2006, 2008), Liang & Zhang (2006), Kann, Klose & Zeh (2006), found a remarkable clustering

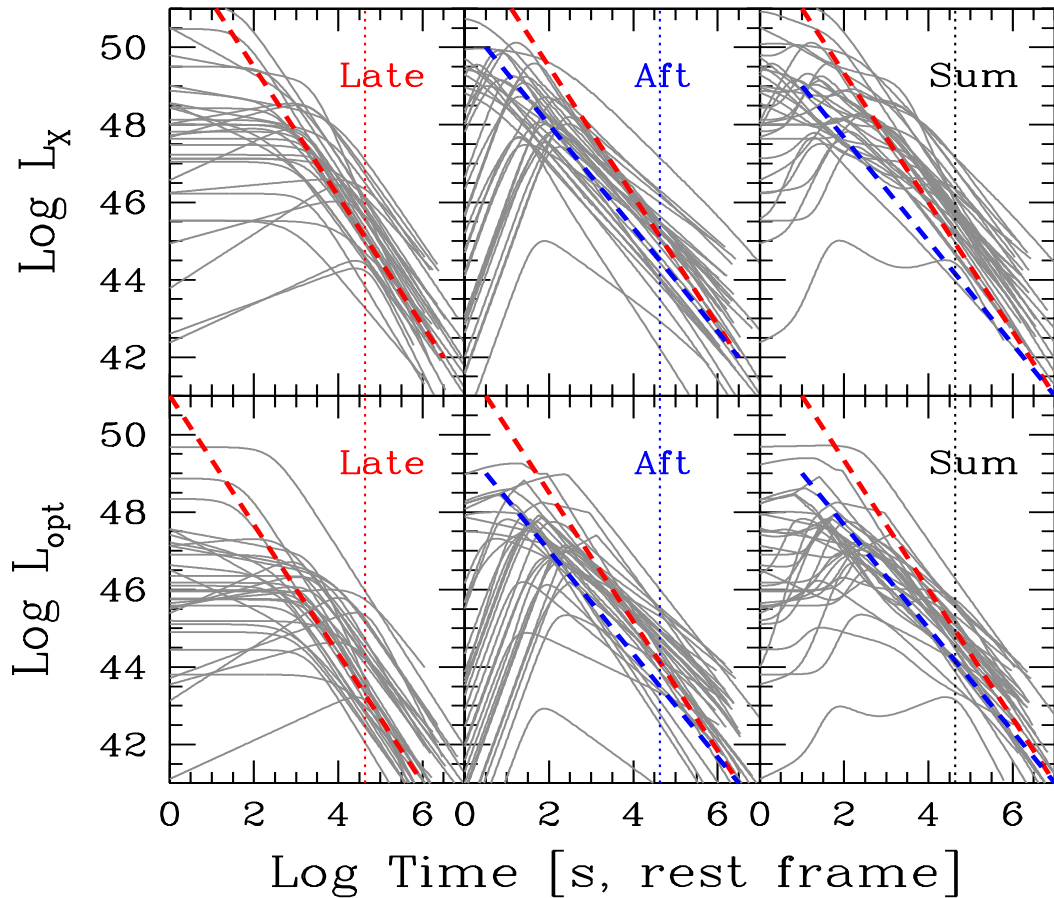


Figure 17. The light curves, as inferred from the modelling, for the 33 GRBs in the X-ray (top panels) and optical (bottom panels) bands. The late prompt (left panels), afterglow (middle panels) and total (left panels) emission are shown. The vertical dotted lines correspond to 12 hours. Note that the total optical luminosity at 12 hours is more clustered than the late prompt and afterglow luminosities. The dashed lines in the left panels correspond to $L \propto t^{-5/3}$, while in the middle and right panels also decays $L \propto t^{-5/4}$ are shown for reference.

of the optical luminosities around two well separated values. However the total optical luminosities (right bottom panel of Fig. 17) are more dispersed than the afterglow ones (middle bottom panel).

Our scenario makes some predictions and calls for some consistency checks. We are analysing in more details the data for the GRBs of the present sample to find confirmation of and/or problems with our scenario, and the results will be presented in a forthcoming paper (Nardini et al., in preparation). The main obvious prediction concerns the presence or absence of jet breaks. When both the X-ray and optical light curves are late-prompt dominated, no jet break should be seen. Viceversa, when they are both dominated by the afterglow emission, an achromatic jet break is expected (even if the after-break slope may be shallower). A chromatic jet break should be observed when only one of the two spectral bands is dominated by the afterglow flux. We stress that well sampled data are required to reliably assess the relative contribution of the two components.

A further general prediction concerns the spectral shape of the late prompt flux. In order for it to be negligible with respect to the the afterglow optical emission, there must be a spectral break between the optical and X-ray bands, and the slope below the break should be rather flat. From our modelling some GRBs require that

either this slope is extremely hard or there is a break within the X-ray band (or both). We plan to re-analyse the data of these bursts, looking for evidence of either a break in the X-ray spectrum, or a very hard optical spectrum (this will depend on the assumed optical extinction). This will impact also on the assumed value of the N_{H} derived by fitting the X-ray data with a simple power-law model.

In our scenario the observed optical and X-ray fluxes can be often ascribed to different processes. Therefore, when analysing the simultaneous optical to X-ray spectral energy distribution, some caution should be made in interpreting it as a single component connecting the optical and X-ray data. This has to be consistent with the analysis of the entire light curve in both bands, to be confident that they are produced by the same process. Only in such cases the host galaxy dust extinction can be compared to the X-ray absorption. Spectral information from NIR to UV would be crucial to this goal.

6 ACKNOWLEDGEMENTS

Financial support was partly provided by a PRIN-INAF 2008 and the ASI I/088/06/0 grants. This work made use of data supplied by the UK Swift Science Data Centre at the University of Leicester.

APPENDIX A: PHOMETRIC DATA REFERENCES

References of the photometric data plotted in Figs. 1, 2, 3, 4, 5, 6, 7, 8, 9, 16.

- GRB 050318: Still et al. (2005);
- GRB 050319: Woźniak et al. (2005), Mason et al. (2006), Quimby et al. (2006), Huang et al. (2007), Kamble et al. (2007);
- GRB 050401: Rykoff et al. (2005), De Pasquale et al. (2005), Watson et al. (2006), Kamble et al. (2008);
- GRB 050408: Foley et al. (2006), de Ugarte Postigo et al. (2007);
- GRB 050416a: Holland et al. (2007), Soderberg et al. (2007);
- GRB 050525a: Torii & BenDaniel (2005); Malesani et al. (2005), Chiang et al. (2005), Mirabal, Bonfield & Schawinski (2005), Homewood et al. (2005), Haislip et al. (2005), Green et al. (2005), Klotz et al. (2005a), Blustin et al. (2006);
- GRB 050730: Sota et al. (2005), Holman, Garnavich & Stanek (2005), Burenin et al. (2005), Klotz et al. (2005b), D’Elia et al. (2005a), Bhatt & Sahu (2005), Kannappan et al. (2005), Pandey et al. (2006);
- GRB 050801: Monard (2005), Fynbo et al. (2005c), Rykoff et al. (2006);
- GRB 050802: Pavlenko et al. (2005), Fynbo et al. (2005e), Oates et al. (2007);
- GRB 050820a: Cenko et al. (2006a);
- GRB 050824: Sollerman et al. (2007);
- GRB 050922c: Norris et al. (2005), Jakobsson et al. (2005b), Andreev & Pozanenko (2005), Durig & Price (2005), Henych et al. (2005), Novak (2005), Piranomonte et al. (2005), D’Elia et al. (2005b), Covino et al. (2005), Li et al. (2005);
- GRB 051111: Butler et al. (2006), Yost et al. (2007);
- GRB 060124: Romano et al. (2006), Misra et al. (2007);
- GRB 060206: Woźniak et al. (2006), Stanek et al. (2007), Curran et al. (2007a);
- GRB 060210: Stanek et al. (2007), Curran et al. (2007b), Cenko et al. (2008);
- GRB 060418: Melandri et al. (2006a), Cobb (2006a), Jelínek Kubánek & Prouza (2006), Koppelman (2006), Chen et al. (2006), Hafizov et al. (2006), Karimov (2006), Molinari et al. (2007);
- GRB 060512: Mundell & Steele (2006), Cenko (2006a), Milne (2006), De Pasquale & Cummings (2006), Cenko & Baumgartner (2006), Sharapov Djupvik & Pozanenko (2006);
- GRB 060526: Campana et al. (2006b), French & Jelinek (2006), Covino et al. (2006), Lin et al. (2006), Brown et al. (2006), Khamitov et al. (2006a), Morgan & Dai (2006), Khamitov et al. (2006b), Rumyantsev & Pozanenko (2006), Kann & Hoegner (2006), Khamitov et al. (2006c), Baliyan et al. (2006), Khamitov et al. (2006d), Khamitov et al. (2006e), Terra et al. (2006), Khamitov et al. (2006f), Rumyantsev et al. (2006), Dai et al. (2007), Thöne et al. (2008);
- GRB 060614: French et al. (2006), Schmidt Peterson & Lewis (2006), Cobb et al. (2006), Fynbo et al. (2006b), Della Valle et al., (2006), Gal-Yam et al. (2006), Mangano et al. (2007b);
- GRB 060729: Grupe et al. (2007);

- GRB 060904b: Skvarc (2006), Oates & Grupe (2006), Mescheryakov et al. (2006), Cobb & Bailyn (2006), Greco et al. (2006), Soyano Mito & Urata (2006), Huang et al. (2006), Asfandyarov Ibrahimov & Pozanenko (2006), Klotz et al. (2008);
- GRB 060908: Nysewander et al. (2006), Antonelli et al. (2006), Morgan et al. (2006), Cenko et al. (2008);
- GRB 060927: Guidorzi et al. (2006), Torii (2006a), Ruiz-Velasco et al. (2007);
- GRB 061007: Mundell et al. (2007);
- GRB 061121: Page et al. (2006), Melandri et al. (2006b), Uemura Arai & Uehara (2006), Marshall Holland & Page (2006), Halpern Mirabal & Armstrong (2006a), Cenko (2006b), Torii (2006b), Halpern Mirabal & Armstrong (2006b), Efimov Rumyantsev & Pozanenko (2006a), Halpern & Armstrong (2006a), Halpern & Armstrong (2006b), Efimov Rumyantsev & Pozanenko (2006b), Cobb (2006b);
- GRB 061126: Perley et al. (2008a), Gomboc et al. (2008);
- GRB 070110: Malesani et al. (2007), Troja et al. (2007);
- GRB 070125: Cenko & Fox (2007), Xing et al. (2007), Uemura Arai & Uehara (2007), Greco et al. (2007), Yoshida Yanagisawa & Kawai (2007), Terra et al. (2007), Mirabal Halpern & Thorstensen (2007), Updike et al. (2008), Chandra et al. (2008);
- GRB 071003: Perley et al. (2008b), Cenko et al. (2008);
- GRB 071003: Covino et al. (2008a); Cenko et al. (2008);
- GRB 080310: Milne & Williams (2008a), Covino et al. (2008b), Chen et al. (2008), Garnavich Prieto & Pogge (2008a), Yoshida et al. (2008), Kinugasa (2008), Garnavich Prieto & Pogge (2008b), Urata et al. (2008a), Wegner et al. (2008), Hill et al. (2008), Cenko et al. (2008);
- GRB 080319b: Li et al. (2008a), Milne & Williams (2008b), Urata et al. (2008b), Li et al. (2008b), Cwiok et al. (2008), Covino et al. (2008c), Woźniak et al. (2008), Swan Yuan & Rujopakarn (2008), Jelínek et al. (2008), Novak (2008), Krugly Slyusarev & Pozanenko (2008), Perley & Bloom (2008b), Tanvir et al. (2008), Bloom et al. (2008).

REFERENCES

- Antonelli L.A., Covino S., Testi V., 2006, GCN, 5546
 Andreev M. & Pozanenko A., 2005, GCN, 4016
 Asfandyarov I., Ibrahimov M. & Pozanenko A., 2006, GCN, 5741
 Baliyan K.S., Ganesh S., Vats H.O. & Jain J.K., 2006, GCN, 5185
 Beardmore A.P., Osborne J.P., Starling R.L.C., Page K.L., Evans P.A. & Cummings J.R., 2008, GCN, 7399
 Berger E. & Mulchaey J., 2005a, GCN, 3122
 Berger E., Gladders M. & Oemler G., 2005b, GCN, 3201
 Berger E. & Gladders M., 2006, GCN, 5170
 Bhatt B.C. & Sahu D.K., 2005, GCN, 3775
 Bloom J.S., Foley R.J., Kocevski D. & Perley D., 2006, GCN, 5217
 Bloom J.S., Perley D. & Chen H.W., 2006, GCN, 5825
 Bloom J.S., Perley D. & Li W., 2008, ApJ submitted (arXiv:0803.3215v2)
 Blustin A.J., Band D., Barthelmy S., et al., 2006, ApJ, 637, 901
 Burenin R., Tkachenko A., Pavlinsky M., et al., 2005, GCN, 3718
 Burlon D., Ghirlanda G., Ghisellini G., Lazzati D., Nava L., Nardini M. & Celotti A., 2008, ApJ, 685, L19
 Brown P.J., Campana S., Boyd P.T. & Marshall F.E., 2006, GCN, 5172
 Butler N.R., Li W., Perley, D., et al., 2006, ApJ, 652, 1390
 Capalbi M., Malesani D., Perri M. et al., 2007, A&A, 462, 913
 Campana S., Moretti A., Guidorzi C., Chincarini G. & Burrows D.N., 2006a, GCN, 5168
 Campana S., Barthelmy S.D., Burrows D.N., et al., 2006, GCN, 5163
 Cenko S.B., 2006a, GCN, 5125
 Cenko S.B., 2006b, GCN, 5844

- Cenko S.B. & Fox D.B., 2006, GCN, 6028
 Cenko S.B., Kulkarni S.R., Gal-Yam A. & Berger E., 2005, GCN, 3542
 Cenko S.B., Kasliwal M., Harrison F. A., et al., 2006, ApJ, 652, 490
 Cenko S.B., Berger E. & Cohen J., 2006, GCN, 4592
 Cenko S.B., Baumgartner W.H., 2006, GCN, 5156
 Cenko S.B., Kelemen J., Harrison F. A., et al., 2008, ApJ submitted (arXiv:0808.3983)
 Chandra P., Cenko S.B., Frail D.A., 2008, ApJ., 683, 924
 Chen H.W., Thompson I., Prochaska J.X., & Bloom J., 2005, GCN, 3709
 Chen B.A., Lin C.S., Huang K.Y., Ip W.H. & Urata Y., 2006, GCN, 4982
 Chen B.A., Huang L.C., Huang K.Y. & Urata Y., 2008, GCN, 7395
 Chevalier R.A., 1989, ApJ, 346, 847
 Chiang P.S., Huang K.Y., Ip W.H., Urata Y., Qiu Y., & Lou Y.Q. 2005, GCN, 3486
 Chincarini G., Moretti A., Romano P., et al., 2007, ApJ, 671, 1903
 Cobb B.E., 2006a, GCN, 4972
 Cobb B.E., 2006b, GCN, 5878
 Cobb B.E. & Bailyn, C.D., 2006, GCN, 5525
 Cobb B.E., Bailyn, C.D., van Dokkum P.G. & Natarajan P., 2006, ApJ., 651, L85
 Covino S., Piranomonte, S., Fugazza D., Fiore F., Maleani G., Tagliaferri G., Chincarini G. & Stella L., 2005, GCN, 4046
 Covino S., Israel G.L., Ghinassi F. & Pinilla N., 2006, GCN, 5167
 Covino S., D'Avanzo P., Klotz A., et al., 2008a, MNRAS, 388, 347
 Covino S., Tagliaferri G., Fugazza D. & Chincarini G., 2008b, GCN, 7393
 Covino S., D'Avanzo P., Fugazza D. et al., 2008, GCN, 7446
 Cucchiara A., Fox D.B. & Berger E., 2006, GCN, 4729
 Curran P. A., van der Horst A. J., Wijers R.A.M.J., et al., 2007a, MNRAS, 381, L65
 Curran P. A., van der Horst A. J., Beardmore A.P., et al., 2007b, A&A, 467, 1049
 Cusumano G., Mangano V., Angelini L. et al., 2006, ApJ, 639, 316
 Cwiok M., Dominik W., Kasprovicz G., et al., 2008, GCN, 7445
 Dado S., Dar A. & De Rújula A., 2005, ApJ, 646, L21
 D'Elia V., Melandri A., Fiore F., et al., 2005a, GCN, 3746
 D'Elia V., Piranomonte S., Fiore F., et al., 2005b, GCN, 4044
 Dai X., Halpern J.P., Morgan N.D., Armstrong E., Mirabal N., Haislip J.B., Reichart D. E. & Stanek K. Z., 2007, ApJ, 658, 509
 Dainotti M.G., Cardone V.F. & Capozziello S., 2008, MNRAS, 391, L79
 De Pasquale M., Beardmore A.P., Barthelmy S.D., et al., 2006, MNRAS, 365, 1031
 De Pasquale M. & Cummings J., 2006, GCN, 5130
 De Pasquale M., Oates S.R., Page M.J., et al. 2007, MNRAS, 377, 1638
 de Ugarte Postigo A., Fatkhullin T.A., Jhannesson G. et al., 2007, A&A, 462, L57
 Della Valle M., Chincarini G., Panaglia N., et al., 2006, Nature, 444, 1050
 Durig D.T. & Price T., 2005, GCN, 4023
 Efimov Y., Rummyantsev V. & Pozanenko A., 2006a, GCN, 5850
 Efimov Y., Rummyantsev V. & Pozanenko A., 2006b, GCN, 5870
 Eichler, D. & Granot J., 2006, ApJ, 641, L5
 Ellison S.L., Vreeswijk P., Ledoux C., et al., 2006, MNRAS, 372, L38
 Evans P.A., Beardmore A.P. & Page K.L. et al., 2007, A&A, 469, 379
 Evans P.A., Beardmore A.P., Godet O. & Page K.L., 2006, GCN, 5554
 Falcone A.D., Burrows D.N., Morris D., Racusin J., O'Brien P.T., Osborne J.P. & Gehrels N., 2006, GCN, 5009
 Foley R.J., Chen H.W., Bloom J., & Prochaska J.X., 2005, GCN, 3483
 Foley R.J., Perley D.A., Pooley D., et al., 2006, ApJ, 645, 450
 Fox D.B., Berger E., Price P.A. & Cenko S.B., 2007, GCN, 6071
 French J. & Jelinek M., 2006, GCN, 5165
 French J., Melady G., Hanlon L. & Jelinek M., 2006, GCN, 5257
 Fugazza D., D'Avanzo P., Malesani D., 2006, GCN, 5513
 Fynbo J.P.U., Hjorth, J., Jensen, B.L., Jakobsson P., Moller P. & Näränen J., 2005a, GCN, 3136
 Fynbo J.P.U., Jensen, B.L., Hjorth, J. et al., 2005b, GCN, 3176
 Fynbo J.P.U., Jensen B.L., Hjorth J., Woller K.G., Watson D., Fouque P. & Andersen M.I., 2005c, GCN, 3736
 Fynbo J.P.U., Sollerman J., Jensen, B.L., et al., 2005d GCN, 3749
 Fynbo J.P.U., Jensen, B.L., Hjorth, J. et al., 2005e, GCN, 3756
 Fynbo J.P.U., Jensen, Sollerman J., et al., 2005f, GCN, 3874
 Fynbo J.P.U., Limousin M., Castro Cerón J.M., Jensen B.L. & N'ar'anen J., 2006a, GCN, 4692
 Fynbo J.P.U., Watson, D., Thöne C., et al., 2006b, Nature, 444, 1047
 Fynbo J.P.U., Jakobsson P., Jensen, B.L., et al., 2006c, GCN, 5651
 Gal-Yam A., Fox D.B., Price P.A., 2006, Nature, 444, 1053
 Garnavich P., Prieto J.L. & Pogge R., 2008a, GCN, 7409
 Garnavich P., Prieto J.L. & Pogge R., 2008b, GCN, 7414
 Genet F., Daigne F., & Mochkovitch, R., 2007, MNRAS, 381, 732
 Ghirlanda G., Ghisellini G. & Lazzati D., 2004, ApJ, 616, 331
 Ghirlanda G., Nava L., Ghisellini G. & Firmani C., 2007, A&A, 466, 127
 Ghisellini G., Ghirlanda G., Nava L. & Firmani C., 2007, ApJ, 658, L75
 Gomboc A., Kobayashi S., Guidorzi C., et al., 2008, ApJ, 687, 443
 Greco G., Terra F., Bartolini C., et al., 2006, GCN, 5526
 Greco G., Terra F., Bartolini C., et al., 2007, GCN, 6047
 Green D.W.E., Della Valle M., Malesani D., Benetti S., Chincarini G., Stella L., & Tagliaferri G., 2005, IAUC, 8696.1
 Grupe D., Godet O., Barthelmy S., et al., 2006, GCN, 5517
 Grupe D., Gronwall C., Xiang-Yu W., et al., 2007, ApJ, 662, 443
 Guidorzi C., Gomboc A., Kobayashi S., 2007, A&A, 463, 539
 Guidorzi C., Bersier D., Melandri A., et al., 2006, GCN, 5633
 Hafizov B., Sharapov D., Pozanenko A. & Ibrahimov M., 2006, GCN, 4990
 Haislip J., MacLeod C., Nysewander M., et al., 2005, GCN, 3568
 Halpern J.P. & Armstrong E., 2006a, GCN, 5851
 Halpern J.P. & Armstrong E., 2006b, GCN, 5853
 Halpern J.P., Mirabal N. & Armstrong E., 2006a, GCN, 5840
 Halpern J.P., Mirabal N. & Armstrong E., 2006a, GCN, 5847
 Hill G., Prochaska J.X., Fox D., Schaefer B. & Reed M., 2005, GCN, 4255
 Hill J., Ragazzoni R., Baruffolo A. & Garnavich P., 2008, GCN, 7523
 Henych T., Kocka M., Hroch F., Jelinek M. & Hudec R., 2005, GCN, 4026
 Holland S.T., Boyd P.T., Gorosabel J., et al., 2007, AJ, 133, 122
 Holman M., Garnavich P., & Stanek K.Z., 2005, GCN, 3716
 Homewood A., Hartmann D.A., Garimella K., Henson G., McLaughlin J., & Brimeyer A., 2005, GCN, 3491
 Huang K.Y., Ip W.H., Lee Y.S. & Urata Y., 2006, GCN, 5549
 Huang K.Y., Urata Y., Kuo P. H. et al., 2007, ApJ, 654, L25
 Ioka K., Toma K., Yamazaki R. & Nakamura T., 2006, A&A, 458, 71
 Jakobsson P., Fynbo J.P.U., Paraficz D., Telting J., Jensen B.L., Hjorth J. & Castro Cerón J.M., 2005a, GCN, 4029
 Jakobsson P., Paraficz D., Telting J., Fynbo J.P.U., Jensen B.L., Hjorth J. & Castro Cerón J.M., 2005b, GCN, 4015
 Jaunsen A.O., Malesani D., Fynbo J.P.U., Sollerman J. & Vreeswijk P.M., 2007, GCN, 6010
 Jelínek M., Kubánek P. & Prouza M., 2006, GCN, 4976
 Jelínek M., Castro-Tirado A.J., Chantry V. & Plá J., 2008, GCN, 7476
 Kamble A., Resmi L. & Misra K., 2007, ApJ, 664, L5
 Kamble A., Misra K., Bhattacharya D. & Sagar R., 2008, MNRAS submitted (arXiv0806.4270K)
 Kann D.A. & Hoegner C., 2006, GCN, 5182
 Kann D. A., Klose S., Zeh A., 2006, ApJ, 641, 993
 Kann D.A., Klose S., Zhang B. et al., 2008, ApJ submitted (2007arXiv0712.2186K)
 Kannappan S., Garnavich P., Stanek K.Z., Christlein D. & Zaritsky D., 2005, GCN, 3778
 Karimov R., Hafizov B., Pozanenko A. & Ibrahimov M., 2006, GCN, 5112
 Kennea J.A., Burrows D.N., Goad M., Norris J. & Gehrels N., 2005, GCN, 4022
 Khamitov I., Bikmaev I., Sakhbullin N., et al., 2006a, GCN, 5173
 Khamitov I., Bikmaev I., Sakhbullin N., et al., 2006b, GCN, 5177
 Khamitov I., Bikmaev I., Sakhbullin N., et al., 2006c, GCN, 5183
 Khamitov I., Bikmaev I., Sakhbullin N., et al., 2006d, GCN, 5186
 Khamitov I., Bikmaev I., Sakhbullin N., et al., 2006e, GCN, 5189
 Khamitov I., Bikmaev I., Sakhbullin N., et al., 2006f, GCN, 5193
 Kinugasa K., 2008, GCN, 7413
 Klotz A., Bo'ér M., Atteia J.L., Stratta G., Behrend R., Malacrino F. & Damerdjji Y., 2005, A&A, 439, L35
 Klotz A., Bo'ér M., & Atteia J.L., 2005, GCN, 3720
 Klotz A., Gendre B., Stratta, G., et al., 2008, A&A, 483, 847

- Koppelman M., 2006, GCN, 4977
 Krugly Y., Slyusarev I. & Pozanenko A., 2008, GCN, 7519
 Lazzati D., & Perna R., 2007, MNRAS, 375, L46
 Lazzati D., Perna R., & Begelman M.C., 2008, MNRAS, 388, L15
 Li W., Jha S., Filippenko A.V., Bloom J.S., Pooley D., Foley R.J. & Perley D.A., 2005, GCN, 4095
 Li W., Bloom J.S., Chornock R., Foley R.J. Perley D.A. & Filippenko A.V., 2008a, GCN, 7430
 Li W., Chornock R., Perley D.A. & Filippenko A.V., 2008b, GCN, 7438
 Liang E. & Zhang B., 2006, ApJ, 638, 67
 Lin C.S., Huang K.Y., Ip W.H. & Urata Y., 2006, GCN, 5169
 MacFadyen A.I., Woosley S.E. & Heger A., 2001, ApJ, 550, 410
 Mangano V., La Parola V., Cusumano G., et al., 2007a, ApJ, 654, 403
 Mangano V., Holland S.T., Malesani D., et al., 2007b, A&A, 470, 105
 Malesani D., Piranomonte D., Fiore F., Tagliaferri G., Fugazza D., & Cosentino R., 2005, GCN, 3469
 Malesani D., Fynbo J.P.U., Jaunsen A.O. & Vreeswijk P.M., 2007, GCN, 6021
 Marshall F.E., Holland S.T. & Page K.L., 2006, GCN, 5833
 Mescheryakov A., Burenin R., Pavlinsky M., et al., 2006, GCN, 5524
 Mason K.O., Blustin A.J., Boyd P. et al. 2006, ApJ, 639, 311
 Melandri A., Gomboc A., Mundell C.G., et al., 2006a, GCN, 4968
 Melandri A., Guidorzi C., Mundell C.G., et al., 2006b, GCN, 5827
 Milne P.A., 2006, GCN, 5127
 Milne P.A. & Williams G.G., 2008a, GCN, 7387
 Milne P.A. & Williams G.G., 2008b, GCN, 7432
 Mirabal N., Bonfield D., & Schawinski K., 2005, GCN, 3488
 Mirabal N., Halpern J. & Thorstensen J.R., 2007, GCN, 6096
 Misra K., Bhattacharya D., Sahu D.K., Sagar R., Anupama G.C., Castro-Tirado A.J., Guziy S.S. & Bhatt B.C., 2007, A&A, 464, 903
 Molinari E., Vergani S.D., Malesani D., et al., 2007, A&A, 469, L13
 Monard B., 2005, GCN, 3728
 Morgan N.D. & Dai X., 2006, GCN, 5175
 Morgan N.D., Vanden Berk, D.E., Brown P. & Evans P.A., 5553
 Morris D., Burrows D., Gehrels N., Greiner J. & Hinshaw D., 2006, GCN, 4694
 Mundell C.G. & Steele I.A., 2006, GCN, 5119
 Mundell C.G., Melandri, A., Guidorzi C., et al., 2007, ApJ., 660, 489
 Nardini M., Ghisellini G., Ghirlanda G., 2006, A&A, 451, 821
 Nardini M., Ghisellini G., Ghirlanda G., 2008, MNRAS, 386, L87
 Nava L., Ghisellini G., Ghirlanda G., Cabrera J.I., Firmani C. & Avila-Reese V., 2007, MNRAS, 377, 1464
 Norris J., Barbier L., Burrows D., et al., 2005, GCN, 4013
 Nousek J.A., Kouveliotou C., Grupe D., et al., 2005, ApJ, 642, 389
 Novak R., 2005, GCN, 4027
 Novak R., 2008, GCN, 4504
 Nysewander M., Reichart D., Ivarsen K., Foster A., LaCluyze A. & Crain J.A., 2006, GCN, 5545
 Oates S. R. & Grupe D., 2006, GCN, 5519
 Oates S. R., de Pasquale M., Page M.J., et al., 2007, MNRAS, 380, 270
 Osip D., Chen H.W. & Prochaska J.X., 2006, GCN, 5715
 Page K.L., Beardmore A.P., Goad M.R., Kennea J.A., Burrows D.N., Marshall F. & Smale A., 2005, GCN, 3837
 Page K.L., Barthelmy S.D., Beardmore A.P., et al. 2006, GCN, 5823
 Page K.L., Willingale R., Osborne J.P., et al., 2007, ApJ, 663, 1125
 Panaitescu A. & Kumar P., 2000, ApJ, 543, 66
 Panaitescu A. & Kumar P., 2001a, ApJ, 554, 667
 Panaitescu A. & Kumar P., 2001b, ApJ, 560, L49
 Panaitescu A. & Kumar P., 2002, ApJ, 571, 779
 Panaitescu A., Mészáros P., Burrows D., Nousek J., Gehrels N., O'Brien P. & Willingale R., 2006, MNRAS, 369, 2059
 Panaitescu A., 2007a, MNRAS, 380, 374
 Panaitescu A., 2007b, MNRAS, 379, 331
 Panaitescu A., 2008, MNRAS, 383, 1143
 Pandey S.B., Castro-Tirado A.J., McBreen S., et al., 2006, A&A, 460, 415
 Pavlenko E., Efimov Y., Shlyapnikov A., Baklanov A., Pozanenko A. & Ibrahimov M., 2005, GCN, 3744
 Pe'er A., Mészáros P. & Rees M.J., 2006, ApJ, 652, 482
 Perley D.A., Chornock R., Bloom J.S., Fassnacht C. & Auger M.W., GCN, 6850
 Perley D.A., Bloom J.S., Butler J.S., et al., 2008a, ApJ, 672, 449
 Perley D.A. & Bloom J.S., 2008a, GCN, 7406
 Perley D.A., Li, W., Chornock R., et al., 2008b, ApJ submitted (arXiv:0805.2394v2)
 Perley D.A. & Bloom J.S., 2008b, GCN, 7535
 Perri M., Giommi P., Capalbi M. et al. 2005, A&A, 442, L1
 Perri M., Guetta D., Antonelli L.A., et al., 2007, A&A, 471, 83
 Piranomonte S., Magazzu A., Mainella G., et al., 2005, GCN, 4032
 Price P.A., Berger E. & Fox D.B., 2006, GCN, 5275
 Prochaska J.X., Bloom J.S., Wright J.T., Butler R.P., Chen H.W., Vogt S.S. & Marcy G.W., 2005, GCN, 3833
 Prochaska J.X., Chen H.W., Bloom J.S., Falco E., Dupree A.K., 2006, GCN, 5002
 Prochaska J.X., Perley D.A., Modjaz M., Bloom J.S., Poznanski, D. & Chen H.-W., 2007, GCN, 6864
 Prochaska J.X., Murphy M., Malec A.L. & Miller K., 2008, GCN, 7388
 Quimby R. M., Rykoff E. S., Yost S. A. et al., 2006, ApJ, 640, 402
 Racusin J.L., Karpov S.V., Sokolowski M. et al., 2008, Nature, 455, 183
 Rol E., Jakobsson P., Tanvir N. & Levan A., 2006, GCN, 5555
 Romano P., Campana S., Chincarini G., et al., 2006, A&A, 456, 917
 Ruffini R., Bernardini M.G., Bianco C.L., et al., 2008, Proc. of the XI Marcel Grossmann Meeting, Berlin (Germany), in press (astro-ph/0804.2837)
 Ruiz-Velasco A.E., Swan H., Troja E., et al., 2007, ApJ., 669, 1
 Rummyantsev V. & Pozanenko A., 2006, GCN, 5181
 Rummyantsev V., Pozanenko A., Ibrahimov M. & Asfandyarov I., 2006, GCN, 5306
 Rykoff E. S., Yost S. A., Krimm H. A. et al., 2005, ApJ, 631, L121
 Rykoff E. S., Mangano V., Yost S. A., et al., 2006, ApJ, 638, L5
 Schady P., Mason K.O., Page M.J., et al., 2007, MNRAS, 377, 284
 Schlegel D.J., Finkbeiner D.P. & Davis M., 1998, ApJ, 500, 525
 Schmidt B., Peterson B. & Lewis K., 2006, GCN, 5258
 Shao L. & Dai Z.G., 2007, ApJ, 660, 1319
 Shao L., Dai Z.G. & Mirabal N., 2008, ApJ, 675, 507
 Sharapov D., Djupvik A. & Pozanenko A., 2006, GCN, 5267
 Skvarc J., 2006, GCN, 5511
 Soderberg A.M., Nakar E., Cenko S.B., et al., 2007, ApJ, 661, 982
 Sollerman J., Fynbo, J.P.U., Gorosabel J., et al., 2007, A&A, 466, 839
 Sota A., Castro-Tirado A.J., Guziy S., Jelinek M., de Ugarte Postigo A., Gorosabel J., Bodganov A., & Pérez-Ramírez M.D., 2005, GCN, 3705
 Soyano T., Mito H. & Urata Y., 2006, GCN, 5548
 Stanek K.Z., Dai X., Prieto J.L., et al., 2007, ApJ, 654, L21
 Still M., Roming P. W. A., Mason, K. O. et al. 2005, ApJ, 635, 1187
 Swan H., Yuan F. & Rujopakarn W., 2008, GCN, 7470
 Tagliaferri G., Goad M., Chincarini G., et al., 2005, Nature, 436, 985
 Tanvir N.R., Perley D.A., Levan A.J., Bloom J.S., Fruchter A.S. & Rol E., 2008, GCN, 7621
 Terra F., Greco G., Bartolini C., et al., 2006, GCN, 5192
 Terra F., Greco G., Bartolini C., et al., 2007, GCN, 6064
 Thöene C.C., Levan A., Jakobsson P., et al., 2006 GCN, 5373
 Thöene C.C., Kann D.A., Johannesson G., et al., 2008, A&A submitted (arXiv:0806.1182v1)
 Toma K., Ioka K., Yamazaki R. & Nakamura T., 2006, ApJ, 640, L139
 Torii K., & BenDaniel M., 2005, GCN, 3470
 Torii K., 2006a, GCN, 5642
 Torii K., 2006b, GCN, 5845
 Troja E., Cusumano G., O'Brien P. T., et al., 2007, ApJ., 665, L97
 Uemura M., Arai A. & Uehara T., 2006, GCN, 5828
 Uemura M., Arai A. & Uehara T., 2007, GCN, 6039
 Uhm L.Z. & Beloborodov A.M., 2007, ApJ, 665, L93
 Updike A.C., Haislip J.B., Nysewander M.C., et al., 2008, ApJ, in press (arXiv:0805.1094v1)
 Urata Y., Chen T.W., Huang K.Y., Im M. & Lee I., 2008a, GCN, 7415
 Urata Y., Im M., Lee I., Huang K.Y., Zheng W.K. & Xin L.P., 2008b, GCN, 7435

- Vreeswijk P.M., Smette A., Malesani D., Fynbo J.P.U., Jensen B.M., Jakobsson P., Jaunsen A.O. & Ledoux C., 2008, GCN, 7444
- Willingale R., O'Brien P.T., Osborne J.P., et al., 2007, ApJ, 662, 1093
- Watson D., Fynbo J. P. U., Ledoux C. et al., 2006, ApJ, 652, 1011
- Wegner G., Garnavich P., Prieto J.L. & Stanek K.Z., 2008, GCN, 7423
- Woźniak P. R., Vestrand W. T., Wren J. A., White R. R., Evans S. M. & Casperson D., 2005, ApJ, 627, L13
- Woźniak P. R., Vestrand W. T., Wren J. A., White R. R., Evans S. M. & Casperson D., 2006, ApJ, 642, L99
- Woźniak P. R., Vestrand W. T., Wren J. A. & Davis H., 2008, GCN, 7464
- Xing L.P., Zhai M., Qiu Y.L., Wei J.Y., Hu J.Y., Deng J.S., Urata Y. & Zheng W.K., 2007, GCN, 6035
- Yoshida M., Yanagisawa K. & Kawai N., 2007, GCN 6050
- Yoshida M., Yanagisawa K., Shimizu Y., Nagayama S., Toda H. & Kawai N., 2008, GCN, 7410
- Yost S.A., Swan H.F., Rykoff E.S., et al., 2007, ApJ, 168, 925
- Zhang B. & Mészáros P., 2001, ApJ, 552, L35
- Zhang B., Fan Y.Z., Dyks J., et al., 2006, ApJ, 642, 354
- Zhang B., 2007, *Advances in Space Research*, 40, Issue 8, p. 1186 (astro-ph/0611774)
- Zhang W., Woosley S.E. & Heger A., 2007, ApJ, 679, 639